SANDIA REPORT

SAND2021-7815

Printed June 2021

Sandia National Laboratories

Terry Turbopump Expanded Operating Band Modeling and Simulation Efforts in Fiscal Year 2021 Extended Period of Performance – Final Report

Lindsay Gilkey[2], Matthew Solom[3], Bradley Beeny[1], David Luxat[1]

[1] 08852 Severe Accident Analysis Department

[2] 08853 Structural and Thermal Analysis Department

[3] 06812 International Nuclear Security Engineering Department

Sandia National Laboratories

P. O. Box 5800

Albuquerque, New Mexico, 87185-0748

Prepared by
Sandia National Laboratories
Albuquerque, New Mexico
87185 and Livermore,
California 94550

Issued by Sandia National Laboratories, operated for the United States Department of Energy by National Technology & Engineering Solutions of Sandia, LLC.

Available to DOE and DOE contractors from
U.S. Department of Energy
Office of Scientific and Technical Information
P.O. Box 62
Oak Ridge, TN 37831

Telephone: (865) 576-8401
Facsimile: (865) 576-5728
E-Mail: reports@osti.gov
Online ordering: http://www.osti.gov/scitech

Available to the public from
U.S. Department of Commerce
National Technical Information Service
5301 Shawnee Rd
Alexandria, VA 22312

Telephone: (800) 553-6847
Facsimile: (703) 605-6900
E-Mail: orders@ntis.gov
Online order: https://classic.ntis.gov/help/order-methods/

ABSTRACT

This report documents the progress made under the Terry Turbine Expanded Operating Band (TTEXOB) program's modeling and simulation (MODSIM) initiative at Sandia National Laboratories (SNL). It describes the US Federal Fiscal Year 2021 (FY21) extended period-of-performance MODSIM work completed since the closure of FY20 with due reference to the Texas A&M University (TAMU) hybrid milestone 5/6 experimental program. This work, which falls under Milestone 7 of the program, provides a counterpart to the various experiments. The overall TTEXOB program and its milestone-based approach are described in the program's Summary Plan [1]. Details of the individual milestone test plans can be found in the corresponding detailed test plan, e.g. the Milestone 3 and 4 Detailed Test Plan [2]. SNL MODISM is conducted alongside experiments performed at TAMU, and SNL technical staff regularly consults with TAMU on the experimental program. In FY21, MELCOR code models and capabilities were exercised in two different contexts: experimental comparisons to the TAMU ZS-1 and GS-2, and stand-alone analyses of a station black-out (SBO) scenario in a generic boiling water reactor (BWR). Code to experiment comparisons met with fair success when turbine losses were well characterized as for the ZS-1 turbine. Both deterministic and Bayesian calibration processes were used to find a recommended turbine torque multiplier for ZS-1 type turbines. This process could be repeated for GS-2 type turbines if GS-2 losses were better understood. Stand-alone generic BWR SBO calculations revealed that three different modes of self-regulating turbopump behavior may be observed depending on certain modeling parameters and choices having to do with turbine nozzles. Aspects of this predicted behavior may have been observed in TAMU GS-2 experiments.

ACKNOWLEDGEMENTS

The authors would like to thank the major funding stakeholders for their continued support and guidance in this endeavor: the US Department of Energy's Office of Nuclear Energy, the Boiling Water Reactor Owner's Group, and the Institute of Applied Energy. The authors would also like to recognize the assistance, feedback, and input from the Terry Turbine User Group supported through the Electric Power Research Institute's Nuclear Maintenance Application Center. Further, the authors would like to acknowledge the faculty, staff, and students at Texas A&M University for their hard work and steadfast commitment to this effort.

CONTENTS

LIST OF FIGURES

LIST OF TABLES

This page left blank

EXECUTIVE SUMMARY

This report documents the progress made under the Terry Turbine Expanded Operating Band (TTEXOB) program's modeling and simulation (MODSIM) initiative at Sandia National Laboratories (SNL). It describes the US Federal Fiscal Year 2021 (FY21) extended period-of-performance MODSIM work completed since the closure of FY20 with due reference to the Texas A&M University (TAMU) hybrid milestone 5/6 experimental program. This work, which falls under Milestone 7 of the program, provides a counterpart to the various experiments. The overall TTEXOB program and its milestone-based approach are described in the program's Summary Plan [1]. Details of the individual milestone test plans can be found in the corresponding detailed test plan, e.g. the Milestone 3 and 4 Detailed Test Plan [2]. SNL MODISM is conducted alongside experiments performed at TAMU, and SNL technical staff regularly consults with TAMU on the experimental program. In FY21, MELCOR code models and capabilities were exercised in two different contexts: experimental comparisons to the TAMU ZS-1 and GS-2, and stand-alone analyses of a station black-out (SBO) scenario in a generic boiling water reactor (BWR). Code to experiment comparisons met with fair success when turbine losses were well characterized as for the ZS-1 turbine. Both deterministic and Bayesian calibration processes were used to find a recommended turbine torque multiplier for ZS-1 type turbines. This process could be repeated for GS-2 type turbines if GS-2 losses were better understood. Stand-alone generic BWR SBO calculations revealed that three different modes of self-regulating turbopump behavior may be observed depending on certain modeling parameters and choices having to do with turbine nozzles. Aspects of this predicted behavior may have been observed in TAMU GS-2 experiments.

ACRONYMS AND DEFINITIONS

Abbreviation	Definition
1F2	Fukushima Daiichi Unit 2
BDBE	Beyond Design Basis Event
BWR	Boiling Water Reactor
CF	Control Function
CST	Condensate Storage Tank
CVH	Control Volume Hydrodynamics
CY	Calendar Year
DAQ	Data Acquisition
DC	Direct Current
DOE	U.S. Department of Energy
DOE-NE	U.S. Department of Energy's Office of Nuclear Energy
EPRI	Electric Power Research Institute
FL	Flow Path
FY	Fiscal Year
IAE	Institute of Applied Energy
INL	Idaho National Laboratory
MODSIM	Modeling and Simulation
MSL	Main Steam Line
NHTS	Nuclear Heat Transfer Systems
P&ID	Piping and Instrumentation Diagram
PIV	Particle Image Velocimetry
PRA	Probabilistic Risk Assessment
PWR	Pressurized Water Reactor
RCIC	Reactor Core Isolation Cooling
RPV	Reactor Pressure Vessel

Abbreviation	Definition
SC	Sensitivity Coefficient
SNL	Sandia National Laboratories
TAMU	Texas A&M University
TDAFW	Turbine Driven Auxiliary Feedwater
TTEXOB	Terry Turbine Expanded Operating Band Committee
TTUG	Terry Turbine User Group
Turbo-TAG	Nuclear Grade Terry Turbopump Advisory Group
VFD	Variable Frequency Drive

1. INTRODUCTION

This report documents the progress made under the Terry Turbine Expanded Operating Band (TTEXOB) program's modeling and simulation (MODSIM) initiative at Sandia National Laboratories (SNL). It describes the US Federal Fiscal Year 2021 (FY21) extended period-of-performance MODSIM work performed since the closure of FY20 with due reference to the Texas A&M University (TAMU) hybrid milestone 5/6 experimental program. This work, which falls under Milestone 7 of the program, provides a counterpart to the various experiments. The overall TTEXOB program and its milestone-based approach are described in the program's Summary Plan [1]. Details of the individual milestone test plans can be found in the corresponding detailed test plan, e.g. the Milestone 3 and 4 Detailed Test Plan [2]. SNL MODISM is conducted alongside experiments performed at TAMU, and SNL technical staff regularly consults with TAMU on the experimental program.

The testing at TAMU is – as of mid-FY21 - supported by two primary groups: the U.S. Department of Energy (DOE) largely through SNL and Idaho National Laboratory (INL), and the U.S. nuclear industry. Formerly, Japan's Ministry of Economy, Trade, and Industry – by way of the Institute of Applied Energy (IAE) – was a source of support as outlined in the project's charter [3].

Details on the experimental work have previously been reported to the IAE [4] in alignment with the Japanese fiscal year and subsequently to the DOE [5] in alignment with the US fiscal year. This report for FY21 builds upon the experimental and MODSIM progress reported in prior fiscal years [6], [7], [8], [14], [18], [19], [20], [25].

Results and analyses introduced here are expected to be disseminated in relevant scientific and industrial publications and conferences such as the Terry Turbine Users Group (TTUG) [9]. Journal publications have already come out of the past fiscal years [10], [11], and future publications are expected.

1.1. Background

Prior to the accidents at the Fukushima Daiichi Nuclear Power Plant, assumptions about and modeling of Terry turbopump performance came mostly from generic vendor operational limits based on the National Electrical Manufacturers Association standard SM23 *Steam Turbine for Mechanical Drive Service* [12] established for turbines intended to deliver continuous reliable service with little or no maintenance. The standard has since been deemed obsolete and was withdrawn.

The Reactor Core Isolation Cooling (RCIC)/Turbine-Driven Auxiliary Feedwater (TDAFW) system performance under beyond design basis event (BDBE) conditions is poorly known and is largely based on conservative assumptions used in probabilistic risk assessment (PRA) applications. For example, common PRA practice holds that battery power (DC) is required for RCIC operation to control the reactor pressure vessel (RPV) water level, and that a loss of DC power results in RCIC flooding of the steam lines with an assumed subsequent failure of the RCIC system. This assumption for accident analysis implies that RCIC operation should terminate on battery depletion, which is conservatively estimated to range from 4 to 12 hours. In contrast, real-world observations from Fukushima Daiichi Unit 2 (1F2) show that RCIC function was affected but not terminated by uncontrolled steam line flooding, and in fact provided coolant injection for nearly three days [13], [14], [15], [16].

Use of conservative assumptions regarding equipment function limits the possible mitigation options for normal and emergency operations. Even in the PRA application space, a best-estimate approach via mechanistic modeling may be a preferable alternative to conservative assumptions. Improved understanding of Terry turbopumps can be realized through an iterative process of advanced modeling and full-scale experimental testing.

The events at Fukushima Daiichi, qualitative analysis, and experience in other industries demonstrate the Terry turbopump has significantly greater operating flexibility than credited in nuclear power plant operations. In particular, operating experience indicates that the Terry turbopump system was qualified for plant operations only to a small subset of its capability. Defining (expanding) this operating band through modeling and testing provides operational flexibility to preclude the occurrence of core damage events such as those that occurred at Fukushima Daiichi with minimal cost to the fleet of plants (i.e., update the operations procedures and train staff on its capability).

The RCIC systems in Fukushima Daiichi Units 2 and 3 operated for extended time periods of up to 68 hours under various RPV pressures, poor steam quality, and with high lube oil and suction temperature values. Data indicates that the Terry turbopump also ran in a 'self-regulating' mode; steam quality impacted the turbine speed such that RPV make-up maintained a relative steady level without any electronic control feedback [13], [14].

The Terry turbopump is used in a wide variety of commercial applications which are not as well controlled as the nuclear industry design limits. The history of the Terry turbopump dates back to the early 1900's and it has a reputation for reliable and rugged performance under a broad range of operating conditions. It is commonly known within other commercial industries that the Terry turbopump can run with water ingestion into the turbine [14]. In addition, a turbine qualification test was run at extreme conditions including ingestion of a large slug of water showing no loss of function or damage to the turbine [17].

Based on the experiences at Fukushima and the nuclear industry at large, the Terry turbopump system is hypothesized to have the capability to operate for days or weeks over an extended range of steam pressures, steam conditions, and increased lube oil temperature conditions with limited to no active control features.

1.2. TTEXOB Program Approach – Review and Summary

The TTEXOB program, guided by the Nuclear Terry Turbopump Advisory Group (Turbo-TAG), uses a milestone approach to define the true operating limitations (margins) of the Terry turbopumps used in the nuclear industry. Milestones 2 through 6 are described in the FY20 report [25]. Hybrid Milestone 5&6 - a replacement for the former Milestone 5 and Milestone 6 – is briefly explained below as is Milestone 7.

1.2.1. Hybrid Milestone 5&6

Hybrid Milestone 5&6 is a compromise aimed at replacing both Milestone 5 and Milestone 6. Hybrid Milestone 5&6 endeavors to explore – without full-scale steam and steam/water testing:

1. Scaling effects/factors, and
2. Terry turbopump self-regulation

Knowledge gaps include:

- Full-scale steam test data,
- Full-scale duration test with steam,
- Self-regulation (full-scale), and
- Impact of steam quality

To deal with the question of scaling effects/factors including full-scale steam test data and full-scale duration:

- GS Terry turbine data will be taken from power plant operation (various inlet pressures, 8 + hours of injection)
- Plant data will be compared to ZS-1 steam test data

To deal with the question of self-regulation, TAMU is running air/water tests with the GS Terry turbine. Possible effects of steam quality will be investigated by expert elicitation.

1.2.2. Milestone 7

The complete suite of MODSIM work complementing all other milestones – including hybrid Milestone 5&6 - is grouped together under Milestone 7. Details on Milestone 7 MODSIM pertaining to Milestones 3 and 4 can be found in [20]. Details on recently completed Milestone 7 MODSIM pertaining to hybrid Milestone 5&6 can be found in the FY20 report [25]. In FY20 and continuing into FY21, Milestone 7 MODSIM for hybrid Milestone 5&6 was two-pronged:

1. MELCOR source code development, and
2. MELCOR input model development and improvement

FY21 saw much more of the latter than the former, as adequate capability for Milestone 7 MODSIM activity was installed by the end of FY20.

2. HYBRID MILESTONE 5&6 PROGRESS – SCALING FACTORS AND SELF-REGULATION

As efforts for Milestones 3 (Full-Scale Separate-Effect Component Experiments) and 4 (Terry Turbopump Basic Science Experiments) concluded, the Turbo-TAG, in conjunction with SNL and INL, identified a suite of full-scale integral experiments required to 'fill in' the remaining parts of the program. Milestone 5 was intended to provide full-scale steam test data and Milestone 6 was intended to study the self-regulating capability of the Terry turbopump in context of an integral experiment. Despite the plans in place for full-scale tests, these milestones were cancelled due to diminished funding across the consortium entities as of (approximately) the beginning of FY20. At that point, there were a few options for moving forward to project conclusion, namely [21]:

- Cease without closing out (no further work or results documentation)
- Cease with closing out (more graceful termination, but with gaps pertaining to full-scale effects and self-regulation still open)
- Defer action on milestones 5 and 6 as they were planned
- Pursue an alternate strategy of addressing gaps targeted by Milestones 5 and 6

The first two options would incur minimal further costs but would jeopardize the integrity of the project as gaps (questions about the applicability of small-scale tests, for example) would remain open and any conclusions drawn about full-scale steam operation and/or self-regulation would come with a lower level of confidence. The option to defer entailed too much uncertainty in the present and a greater ultimate cost in the future if funding did come through for original Milestones 5 and 6. In all likelihood, deferring would have resulted in project cessation without future start-up (thus jeopardizing the integrity of the project due to remaining knowledge gaps). An alternate strategy known as hybrid Milestone 5&6 was the clear preference in view of the circumstances.

2.1. Milestone Overview

The essential goal of hybrid Milestone 5&6 as formulated by the consortium is to obtain a greater level of confidence with respect to the original issues of Milestones 5 and 6. Certain actions that incur comparatively small incremental costs could be taken in order to study scaling effects (original Milestone 5 goals) and self-regulation (original Milestone 6 goals). The components of hybrid Milestone 5&6 include:

- An experimental program exclusively conducted at/by TAMU with existing or gently modified apparatuses (ZS-1, GS-2 air facilities)
- Existing utility experience and resources to include full-scale Terry turbopump operational data (injection of various durations over various inlet pressures)
- ZS-1 steam data obtained by TAMU
- ZS-1 air and air-water self-regulation data obtained by TAMU
- Certain expert elicitation on the issue of the impact of steam quality
- A cost-mitigated spending plan detailing commitments of consortium members

- Milestone 7 type MODSIM activities targeted at:
    - Supporting the new experimental program and/or
    - Leveraging forthcoming experimental data
    - Scaling effects and self-regulation from a MODSIM perspective

SNL – as part of the TTEXOB consortium under the heading of DOE - continued to lend support to TAMU/industry as the experimental program carried on into FY21.

2.2. Milestone Progress

In late FY2020, the Hybrid Milestone 5&6 experimental tasks at Texas A&M University were progressing toward completion. As noted in [25], these tasks included

- Terry ZS-1 steam and steam-water dynamometer-based turbine profiling
- Terry GS-2 air-water uncontrolled feedback testing
- Terry ZS-1 steam and steam-water turbopump profiling, where achievable

Construction on the ZS-1 steam-water test facility in the Laboratory for Nuclear Heat Transfer Systems was completed in FY20 and had performed a limited set of shakedown tests; shakedown testing continued into FY2021. Subsequently, a complete set of steady-state steam-water performance data was collected; this set of data is in the form of points on curves for torque vs. speed, pressure, and steam quality akin to those of the earlier air-water performance curves produced under Milestone 4.

The NHTS ZS-1 test facility is being reconfigured to attempt turbopump profiling tests under dry and wet steam ingestion conditions. The dynamometer will be disconnected from the turbine and a pump will take its place as the turbine's load. The pump's flow will be directed as appropriate for the specific test (e.g., to the steam line feeding the turbine for the uncontrolled feedback tests). This set of turbopump testing is considered a "stretch goal" and may not be achievable within time left to the project.

In addition to ZS-1-based testing, TAMU in FY2021 has designed, constructed, and operated a Terry GS-2-based test loop in the Turbomachinery Laboratory. With input from the TTEXOB and SNL, the loop explored the proposed uncontrolled feedback mode of operation applicable to the RCIC system. In this test apparatus, air is supplied to a mixing vessel that, when supplied with sufficient water, sends a two-phase air-water mixture to the Terry GS-2 employed in prior tests. As was the case in the prior tests, the upper bank of nozzles was blocked off to operate the turbine as a GS-1. Water is separated from the turbine exhaust and redirected to a storage tank for reuse; the remaining air is exhausted to the atmosphere.

The turbine is coupled to both a dynamometer and a pump. The pump draws water from a storage tank and sends it to the mixing tank upstream of the turbine inlet at rates commensurate to its characteristic curve, rotation rate, restrictions, and pressure conditions. The dynamometer allows for additional loading to emulate conditions of greater pump loading than would otherwise exist. The system is fully instrumented and has a large number of individual adjustments to allow for testing under a broad array of conditions.

The primary data collection test runs for uncontrolled feedback in the Turbomachinery Laboratory have been complete. While the data collection for steady-state ZS-1 steam-water profiling and GS-2 uncontrolled feedback has been completed, as of the time of writing the data qualification and data analysis are underway but have yet to be finished. The results of these tests are expected to be published in relevant academic journals.

3. MILESTONE 7 PROGRESS – MELCOR SYSTEMS-LEVEL MODELING AND SIMULATION

MODSIM activities falling under Milestone 7 for FY21 fall into one of two categories: MELCOR source code development and MELCOR input model development. Source code development refers to an addition of:

- Mathematical/physics model(s) to capture physical phenomena, or
- Code capabilities to expand modeling options and/or increase user convenience

Input model development refers to construction of a MELCOR input model meant to represent a given physical system, e.g. an experimental facility or a boiling water reactor (BWR). Input development also encompasses any control logic required to impose a particular experimental condition or plant transient.

A considerable amount of MELCOR source code development aimed at Terry turbopump physics has occurred in recent years (since FY14). However, Milestone 7 MELCOR modeling activities through FY19 did not incorporate those features, and the TTEXOB program has had only limited exposure to them over the last several years. An overview of previous (FY14-FY20) Milestone 7 MODSIM work is given elsewhere [25]. An overview of recent (FY21) Milestone 7 MODSIM work is given here because FY20/FY21 input models use the new systems-level Terry turbopump models/capabilities in order to model both experiments and representative nuclear power plants.

3.1. MELCOR Source Code Development

3.1.1. FY14 through FY20

Beginning in FY14, an independently-funded effort was undertaken – as a complement in parallel with the TTEXOB program - to develop new MELCOR physics models meant to represent the various components of the RCIC Terry turbopump. The models – though designed with the RCIC/TDAFW systems in mind – improved the general usefulness and capability of the MELCOR code. While model development was in progress, the TTUG, the BWR Owners' Group (BWROG), and the TTEXOB consortium were generally made aware of the new MELCOR capabilities including their performance and predictive capability. A comprehensive description of MELCOR models/capabilities added since FY14 is found elsewhere [25]. The list of features includes:

- Homologous pump modeling
- Pelton/Terry turbine pressure stage modeling
- Pelton/Terry turbine velocity stage modeling
- Rigid turboshaft modeling
- Supplemental user-supplied torque terms for pump and rotor models
- Sensitivity coefficient expansions for turbine models
    - Torque multiplier
    - Windage torque term

- An "independent turbine mode" capability

3.1.2. FY21

Apart from minor bug fixes, there was no further required MELCOR development in terms of physics models or capabilities.

3.2. MELCOR Input Model Development

MELCOR input models represent a variety of nuclear and non-nuclear systems. Properly configured, they generate predictions of – among other phenomena - thermal-hydraulic response under steady or transient conditions. MELCOR is generally concerned with radionuclide transport and source term generation but is deployed in this instance for its thermal-hydraulic modeling capabilities which align with an integral, systems-level modeling approach and philosophy.

Through FY19, several MELCOR input models were developed to support Milestone 3 and 4 TAMU experiments, to investigate experimental findings, to identify knowledge gaps, to explore uncertainties, and to ascertain their relative importance in context of an integral analysis. Additionally, MELCOR input models representing nuclear power systems were built to reproduce real-world accident conditions and to learn lessons about code performance and/or accident progression. All MELCOR input models through FY19, however, did not avail themselves of the latest systems-level RCIC models. They resorted instead to user-programmed CF models that suffered from two distinct disadvantages:

- They were not standardized by a formal collection of input structures, and
- They were impenetrable to scrutiny from all users besides the original modeler as they consisted of complicated, interconnected sequences of dozens of CFs

The FY20 MODSIM agenda for Milestone 7 in terms of MELCOR input model development focused on complementing the experimental program of hybrid Milestone 5&6. Previous MELCOR input models (through FY19) that could still reasonably find application given the hybrid Milestone 5&6 agenda were revised and updated to utilize best practices plus the new systems-level RCIC models. As such, the TAMU GS-2 (air) and ZS-1 (air, air/water, steam, steam/water) input models were revised/updated. The 1F2 input model was developed no further. However, a generic BWR input model was developed to demonstrate the new systems-level RCIC models in context of a best-estimate PRA study for risk-informed decision-making. This product is more generally useful (e.g. than 1F2) for several reasons:

- Model shake-down in context of a full reactor model (improves code robustness)
- Lays a foundation for future studies (best-estimate, risk-informed approach)
    - Industry investigating operating procedures or accident management
    - Regulators investigating the level of credit to grant RCIC/TDAFW (perhaps moving away from severe, conservative assumptions)
- More general demonstration of capabilities that users can adapt to fit needs

3.2.1. Overview of Modeling and Simulation Activities (through FY20)

By way of review for SNL MODSIM activities:

- 2015
  - Initial MELCOR input development
  - SNL Solidworks and computational fluid dynamics (CFD) work (Fluent)
- 2016-2018
  - Solidworks and Fluent computations ongoing
  - MELCOR input developments for 1F2, TAMU experiments
  - Analyses to support full-scale testing plan
  - TAMU ZS-1 input model (CF Terry turbine model)
- 2019
  - TAMU ZS-1 and GS-2 (air) input models (CF Terry turbine model)
  - 1F2 input model (CF Terry turbine model)

In FY18, the TAMU ZS-1 input model (CF Terry turbine model) was developed. A main takeaway from MELCOR modeling of ZS-1 experiments was that rotor losses (friction and wheel windage) may be larger and more consequential than initially anticipated. This has obvious implications for the 1F2 model or any other RCIC/TDAFW applications.

In FY19, the TAMU experimental program called for development of a MELCOR GS-2 input model that used air in its turbine. The input model was in several ways similar to that of the ZS-1, but some of the turbine characteristics were different (bigger turbine wheel, different nozzles).

FY20 input development for the TAMU GS-2 and ZS-1 built on the work completed in FY18 and FY19. The FY20 modeling updated the input to utilize the MELCOR systems-level RCIC capabilities.

3.2.2. Recent Input Development (FY21)

Input development proceeded in FY21 for both the TAMU ZS-1 and GS-2 experiment modeling and for the generic BWR with RCIC. The TAMU ZS-1 and GS-2 experiment input decks were developed to include the new RCIC implementation, including a control function that supplied resistive torque. For the generic BWR input development, emphasis was placed on investigating the self-regulating mode of operation during FY21 through input development.

3.2.2.1. Input Development for TAMU ZS-1 and GS-2 Experiments

Section 3.2.1 briefly discussed modeling and simulation activities through FY20 for the TTEXOB. These activities included system-level MELCOR modeling during FY18 through FY20 of the ZS-1 and GS-2 Terry turbine airflow experiments that were performed at TAMU. This modeling is discussed in detail during previous FY18 [19], FY19 [20], and FY20 [25] TTEXOB progress reports. During FY20, the MELCOR input decks originally developed for the FY18 and FY19

modeling of the TAMU ZS-1 and GS-2 Terry turbines were updated to include new model and input developments. The FY21 TAMU ZS-1 and GS-2 model development focused on further development of the input to better represent the experiment and the implementation of loss data from TAMU.

Figure 3.1 show the FY20 MELCOR model/nodalization of the TAMU experiments. Notably, the FY20 implementation included a pump, which was needed at the time as the Terry turbine model required a pump object to output control function quantities such as pump/turbine speed and torque. However, MELCOR source code developments were made during FY20/FY21 that made it so the Terry turbine model could be implemented without a coupled pump object. The turbine torque and speed control function quantities can be pulled from the Terry turbine object using the CVH-TURBTORQ(CV) and CVH-TURBSPD(CV) control functions, respectively. An extra user supplied torque term can be applied to the turbine torque-inertia equation, which supplies a resistive torque in place of a pump. This was implemented to better represent the TAMU air and air-water experiments, which did not include a pump in the facility and instead loaded the turbine with a dynamometer to control turbine speed.

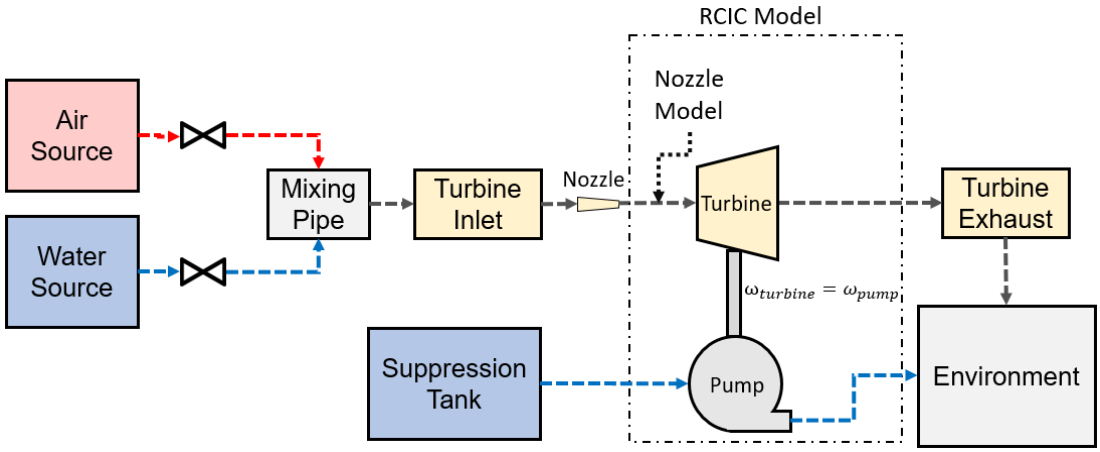

Figure 3.1: FY20 MELCOR model of TAMU experiments with RCIC model.

A visual representation of the FY21 MELCOR modeling and nodalization of the ZS-1 and GS-2 TAMU air and air-water experiments is shown in Figure 3.2. The following methodology was used for modeling the TAMU airflow experiments. For a given flow condition, air tank pressure and temperature were set according to the experimental values. The water source was isolated in the air tests by closing the water source valve. The air tank valve open fraction was adjusted until the model air mass flow rate matched the experimentally observed value. In the case of modeling air-water experiments, the water source valve open fraction was also adjusted to match the experimental value. Once the air and water mass flow rates matched the experimental values, the model's Terry turbine representation was brought up to speed. The modeling used the experiment's dynamometer peak resistive torque to load against the Terry turbine inertia by supplying a dynamometer torque control function to the Terry turbine model in the CV_ROT card.

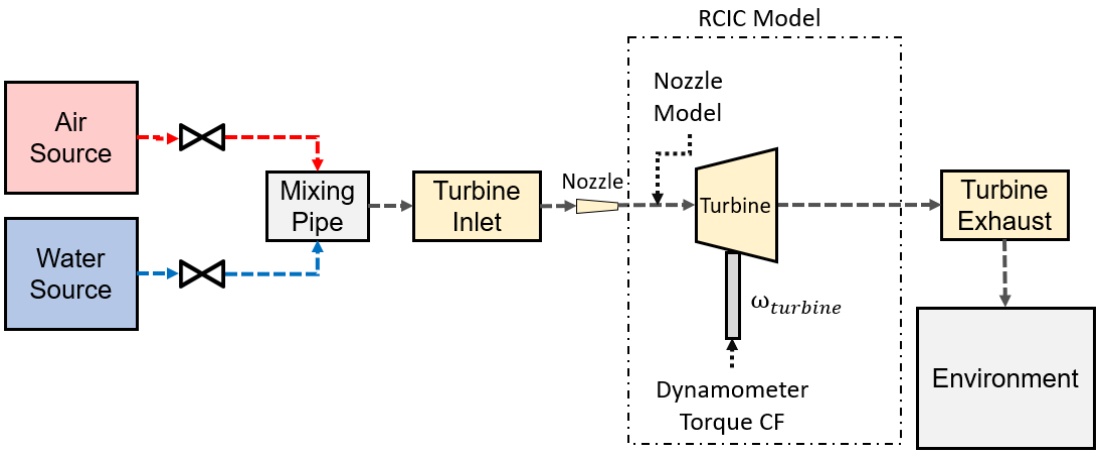

Figure 3.2: Updated FY21 MELCOR model of TAMU experiments with RCIC model.

Other notable input developments for the ZS-1 modeling include a different implementation of the turbine losses. Data obtained from TAMU of the loss magnitude while the ZS-1 Terry turbine was spun in air showed that there is likely a non-negligible linear component of turbine losses in addition to the already known windage component. Data from TAMU was used to fit a curve of the turbine losses as they vary with speed, resulting in the Equation 3.1 for the ZS-1 losses:

$$torque_{loss} = c_{windage}\omega^2 + c_{linear}\omega + constant \tag{3.1}$$

In Equation 3.1, ω is the angular velocity of the turbine wheel, $c_{windage}$ is a loss coefficient scaling the turbine wheel windage, and c_{linear} is a coefficient scaling the linear components of the losses. Previously, it was assumed that the linear component of the turbine losses was negligible compared to the windage term that scales with turbine speed squared. The torque loss term (Equation 3.1) was calculated as a control function in MELCOR and then supplied to the turbine using the CV_REX record.

The net turbine torque equation for the new ZS-1 implementation is then:

$$torque_{net} = c_{torque} \times torque_{turbine} - torque_{loss} \tag{3.2}$$

In Equation 3.2, c_{torque} is a multiplier used to scale the turbine torque, $torque_{turbine}$, as computed from the systems-level velocity stage Terry turbine model. Since this new form assumes the losses have a fixed form and coefficient values, c_{torque} is the calibration coefficient for matching experimental data from TAMU.

Coefficients c_{torque} and loss equation (Equation 3.1) were implemented in the TAMU input using CV_SC 4502 and 4503. For the ZS-1 air tests, the following values were used for the coefficients of Equation 3.1:

Table 3.1: TAMU air test coefficients in Equation 3.1

Coefficient/Constant	Value
$C_{windage}$	1.39×10^{-7}
C_{linear}	2.3×10^{-4}
$constant$	3.8×10^{-2}

3.2.2.2. Input Development for Generic BWR

The generic BWR input deck has been developed for modeling various accident sequences, with an emphasis on capturing the behavior of the RCIC turbopump system. This includes input developments that allow the RCIC system to run without electrical controls in a self-regulating mode of operation. The generic BWR input has been developed extensively from the "base" input that it was originally based upon. These changes and other notable model sensitivities are discussed in this section. Input developments during FY21 built on modifications made in FY20, with emphasis placed on exploring the RCIC turbopump system self-regulating mode of operation, where the RCIC performance was driven by feedback from the RPV level without any electronic control feedback.

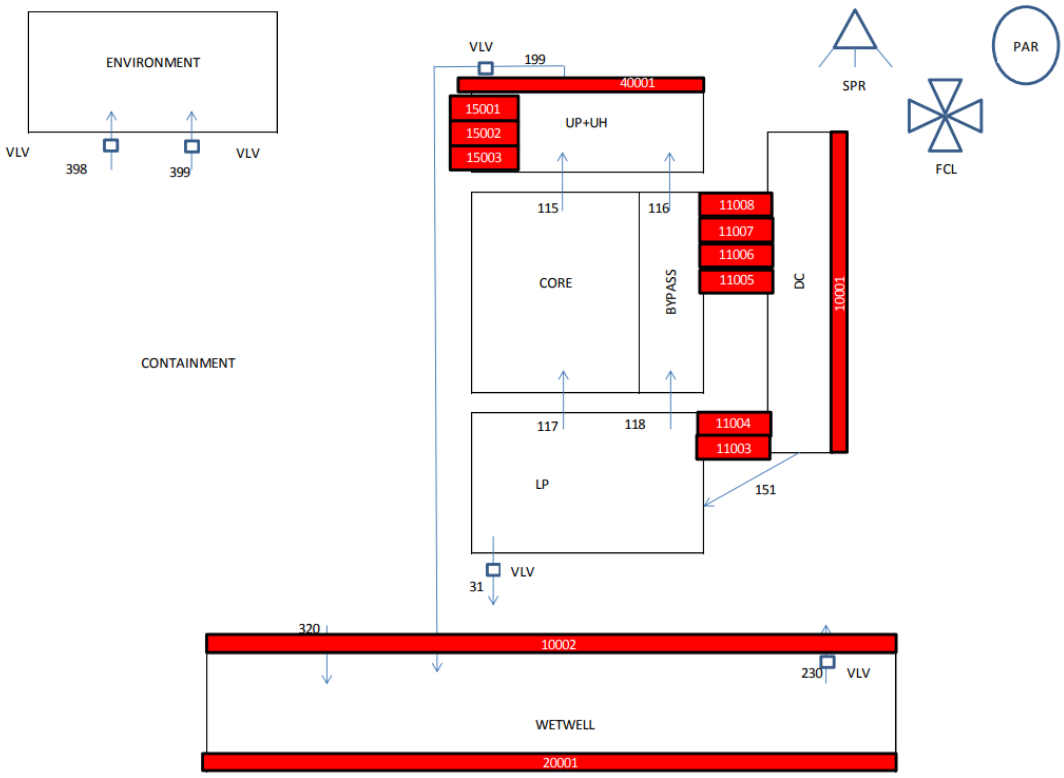

Figure 3.3: Generic BWR nodalization with emphasis on RCIC.

The self-regulating mode of operation for the RCIC Terry turbine is believed to be controlled by the RPV level by the following mechanism. An increase in RPV water level results in degraded steam quality and flooding of the main and RCIC steam lines. This results in water entering the turbine. The degraded steam and water injecting through the nozzles in the RCIC turbine results in diminished turbine performance and less torque being transmitted through the turboshaft to the pump, resulting in decreased pump injection of coolant. This causes the RPV water level to drop and decreases the amount of water entering the RCIC steam line. This, in turn, leads to increased turbine performance, increased injection, a rising RPV water level, and so on.

The RCIC model for the generic BWR uses recent MELCOR code developments described in Section 3.1. This model builds on the one developed for the generic BWR input described in the FY20 report [25] to model self-regulating RCIC operations. In FY20, the generic BWR model was implemented using a MELCOR Terry turbine model object. This was a notable change from the FY19 modeling of Fukushima Daiichi Unit 2, which used a control function model for the RCIC system.

The FY21 modeling entailed changes to parameters such as the pump specifications, turbine mass flow rate, and the turbine scaling coefficients. The intent was to better match available experimental data, CFD data, or operational assumptions.

The RCIC pump and turbine specifications are shown in Table 3.2. These specifications were taken from several sources to construct the generic BWR model, with the main source for the specifications being SAND2015-10662 [14]. These design parameters characterize the RCIC pump and turbine. The RCIC pump was specified to model two-phase pump performance via homologous curve input. The RCIC pump was coupled to the RCIC turbine model to control the pump speed and motor torque using the FL_TSH card in the input deck.

Table 3.2: RCIC Pump and Turbine Base Specifications

Parameter	Value
RCIC Turbine Specifications	
Turbine Radius	0.3048 m
Turbine CV Volume	0.106 m^3
Turbine Moment of Inertia	10.0 kg-m^2
Turbine Friction Torque	10.0 N-m
Turbine Bucket Exit Angle	30º
Turbine Nozzle Diameter	12.7 mm
Number of Nozzles	5
RCIC Pump Specifications	
Rated Pump Speed	4287.0 RPM
Rated Pump Head	7.59 MPa
Rated Pump Torque	448.8 MPa

Parameter	Value
Rated Pump Power	2.0147×10^5 W
Rated Pump Injection Rate	0.03886 m^3/s
Pump Moment of Inertia	30.0 kg-m^2
Other RCIC Related Specifications	
RCIC CF Target Injection Rate	38.733 kg/s
RCIC CF Target Relative Downcomer Level	2.54 m

It was found during the FY21 modeling that some input parameters had significant effects on overall turbopump behavior and performance. For example, the turbine scaling coefficient (sensitivity coefficient SC4502 in MELCOR) had large effects on modeling results. A higher (> 1.0) value results in a higher turbine torque for the same mass flow rate. In one such example input, during controlled operations of RCIC while setting SC4502 to 2.53 (from FY19 GS-2 analysis [20]), a mass flow rate of ~10,000 lbm/hr (4536 kg/hr) steam produced a pump injection of ~39 kg/s. For equivalent pump injection with SC4502 of 1.0, about 18,000 lb/hr (8165 kg/hr) steam flow through the turbine is required. 18,000 lb/hr steam was given by [19] as an appropriate value for controlled RCIC operations, so SC4502 was specified as 1.0 for the most recent model inputs.

Additionally, the GS-1 Terry turbine nozzle height was found to have a significant effect on the behavior of the turbopump system during self-regulation. As noted in the FY20 report [25], adjusting the nozzle height/elevation relative to the steam chest influenced the frequency, magnitude, and duration of turbine speed fluctuations during self-regulation. The nozzle height has a significant effect as the RCIC performance is highly sensitive to the water height in the steam chest, and adjusting the nozzle height will influence how many nozzles are submerged if the steam chest is partially flooded. FY21 modeling efforts revealed that nozzle height is crucial to turbine self-regulation behavior as discussed in Section 3.3.2.

Note that turbine overspeed shutoff is disabled for the present modeling purposes. This is because the turbine will overspeed in the current model soon after the loss of battery power due to the large admittance of steam to the turbine when the RCIC turbine steam line governor and trip valves fail open. The turbine speed will not overshoot again after this initial overspeed. However, prevention of the initial overspeed requires imposition of large magnitude turbine losses that prove disruptive to the remainder of the calculation. Since the present modeling is focused on self-regulation after DC power loss, and since it seems like the turbine in Fukushima Daiichi Unit 2 did not mechanical trip on overspeed, the turbine overspeed RCIC shutoff is currently disabled.

During self-regulation (i.e., no battery power), the only RCIC shutoff implemented in the model is a control function that initiates shutoff if the RCIC pump is aligned to the wetwell after depleting the CST and the wetwell temperature exceeds 373 K. This failure is mechanical in nature, as the RCIC pump will be destroyed by a net loss of positive suction head due to the pump source water temperature.

3.3. MELCOR Modeling Results

The MELCOR modeling results from the TAMU ZS-1 and GS-2 experiments and the generic BWR are discussed in this section.

The TAMU ZS-1 and GS-2 air tests were modeled in MELCOR and compared to experimental data. Emphasis was placed on the ZS-1 modeling as loss data was provided that fixed the form and coefficients of the turbine loss equation. The TAMU ZS-1 air modeling was also selected to demonstrate a Dakota [1] and MELCOR coupling to support integrated uncertainty analysis. A summary of these results and processes are included.

The generic BWR modeling results primarily focus on self-regulation and the way in which different model inputs influence the observed mode of self-regulation. A typical station black-out scenario with DC power loss at two hours into the accident is used for this purpose.

3.3.1. TAMU GS-2 and ZS-1 Modeling Results

The TAMU ZS-1 and GS-2 air experiments were performed at a variety of different turbine speeds and inlet pressures. Quantities such as source temperatures and pressures, mass flow rates, dynamometer torque, turbine speed, turbine torque, and resulting power were collected as part of the experimental process. These quantities were used to develop the input decks for the TAMU experiments in MELCOR. As these models are quick running (typically taking less than five minutes to run to completion), it was feasible to perform a variety of different studies, including uncertainty analysis.

To aid in these studies, a coupling was set up between MELCOR and Dakota. Dakota (Design Analysis Kit for Optimization and Terascale Applications) is a computational toolkit developed at SNL to aid in performing iterative analysis such as parameter studies, calibration, or uncertainty analysis [1] by providing a coupling between algorithms and a driver. The driver is used to set up a workflow:

- pre-process variables sampled iteratively by Dakota,
- update input templates,
- run analysis, and
- perform postprocessing

The FY19 work [20] was performed in part to characterize the TAMU ZS-1 and GS-2 coefficients c_{torque} and $c_{windage}$. However, as net torque is a net product of positive turbine torque and turbine losses, coefficients can be unidentifiable if they are not bounded as there are infinite combinations of quantities of positive torque (which is related to c_{torque}) and turbine losses (which is related to $c_{windage}$) that can yield the same net torque quantity and resulting speed. To implement a more meaningful characterization of the coefficients, additional data on turbine losses was required as it would determine the form of the turbine losses and reduce the problem dimensionality. This was done in FY21 by using the ZS-1 air loss data (see Section 3.2.2.1) and Equation 3.1 with the coefficients in Table 3.1 for the turbine losses. With the loss coefficients determined for the ZS-1 air tests, only c_{torque} was left to calibration via minimization of residuals either on a per experiment basis or on a global basis (by using a least-squares norm).

Figure 3.4 shows the calibrated c_{torque} values derived by minimizing residuals per experiment with a deterministic approach. When using a deterministic approach, the goal is to minimize the

quantity of interest (QOI) residuals. Note that a deterministic approach yields no uncertainty information. Each point on the plot corresponds to a separate Dakota calibration performed per experiment. Several conclusions can be drawn from this plot. First, there appears to be a relationship between the c_{torque} value and the speed. Lower speed experiments generally appear to have a higher calibrated c_{torque} value that decreases as turbine speed is increased. There also appears to be a lesser relationship with pressure; at 70 psia and above, c_{torque} value decreases as pressure increases. It should be noted that the 30 psia and 50 psia results do not follow this same trend. The 50 psia calibrated c_{torque} values decrease as turbine speed increases; however, the c_{torque} vs speed curve does not follow the same pressure trend as observed with the 70 psia and above experiments. It is possible that the 30 and 50 psia experiments exhibit different behavior from the higher pressure experiments as these were performed at lower inlet pressures and mass flow rates, and resulting turbine net torque. Figure 3.5 shows the ZS-1 air test turbine power vs speed curves for the experiments and the calibrated results. Figure 3.6 shows the experimental data vs the MELCOR results for the ZS-1 air data. The calibrated turbine speed residual is almost zero when calibrating on a per experiment basis. The calibrated turbine torque residual is relatively low, but still shifts the power vs speed curve.

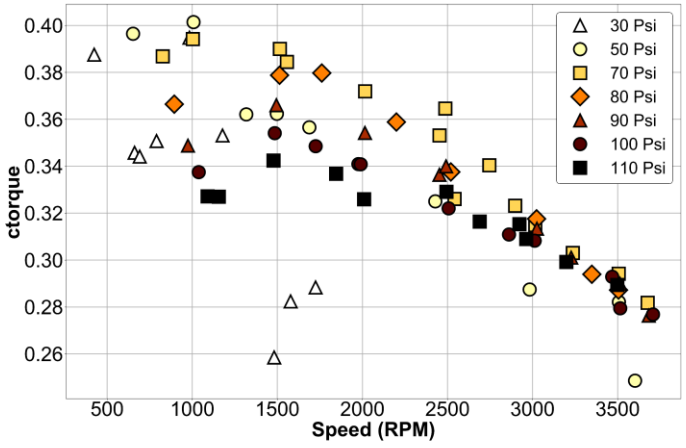

Figure 3.4: Calibrated ctorque values per experiment using a deterministic approach.

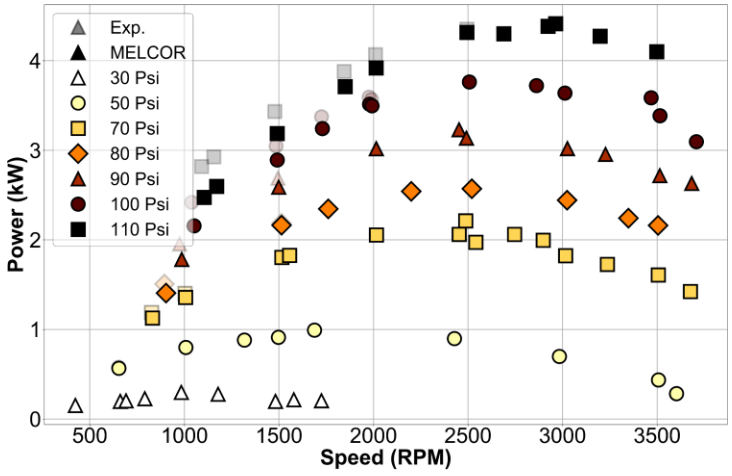

Figure 3.5: ZS-1 air test turbine power vs speed curves for the experiments and the calibrated results using ctorque calibrated per experiment with a deterministic approach.

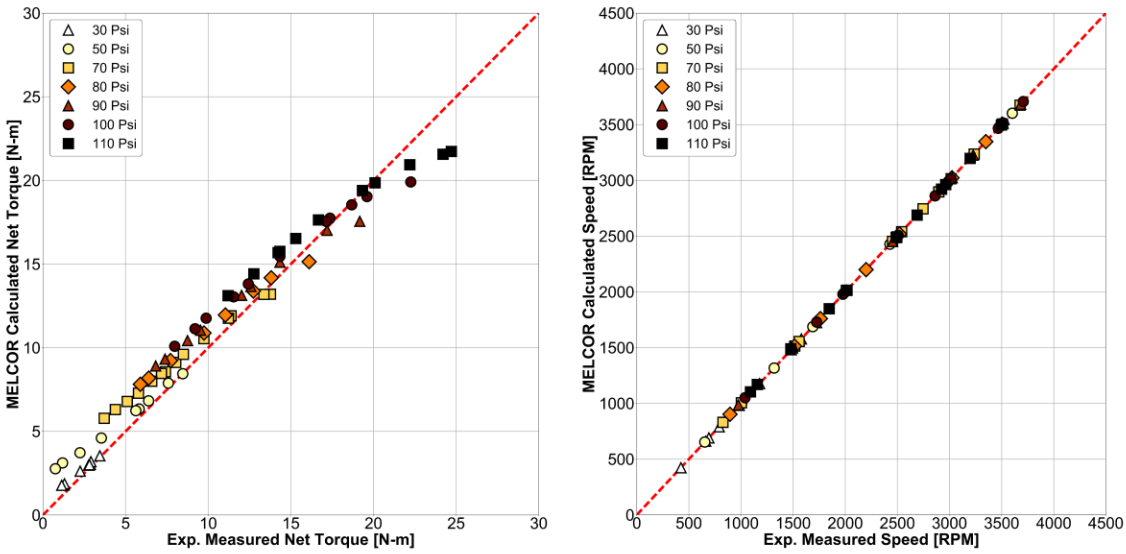

Figure 3.6: The experimental data vs the MELCOR results for the ZS-1 air tests using ctorque calibrated per experiment with a deterministic approach.

The exercise was repeated by calibrating to all experimental data by minimizing the least-square norm of all residuals. Figure 3.7 and Figure 3.8 show the turbine power, speed, and torque results of minimizing the residuals by calibrating c_{torque} using all experimental data with a deterministic approach. The calibrated c_{torque} value was 0.3453, which falls in the range of Figure 3.4.

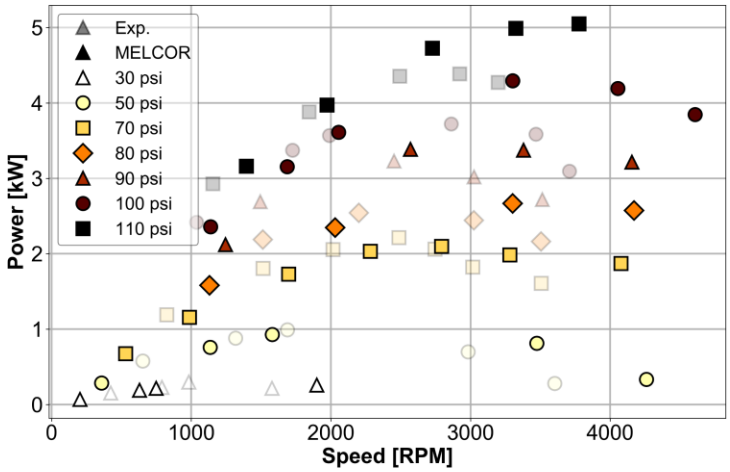

Figure 3.7: ZS-1 air test turbine power vs speed curves for the experiments and the calibrated results using ctorque calibrated with all experiments with deterministic approach.

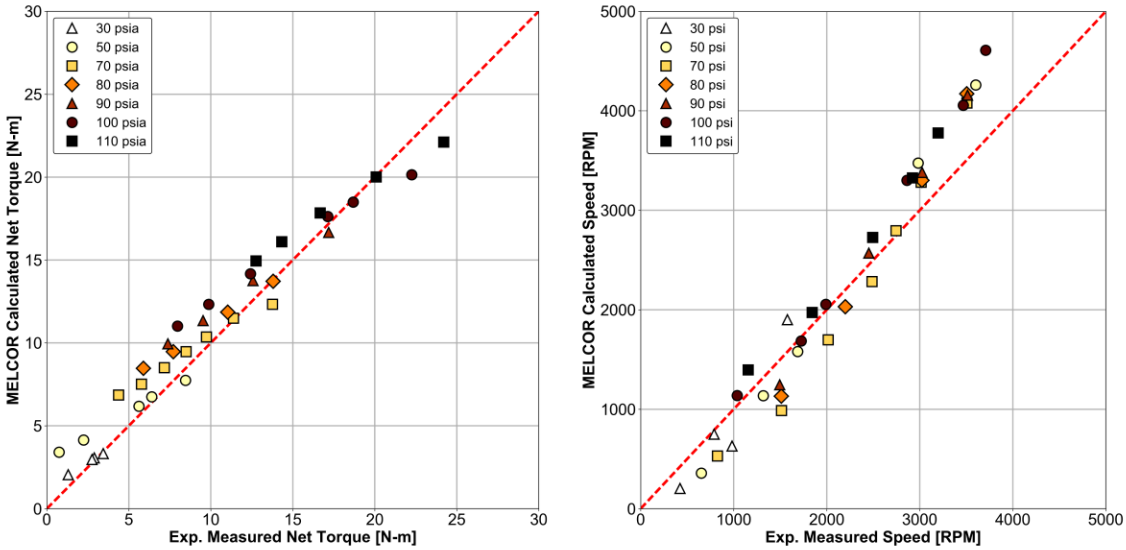

Figure 3.8: The experimental data vs the MELCOR results for the ZS-1 air tests using ctorque calibrated with all experiments with deterministic approach.

Deterministic calibration may be suitable based on the calibration needs, however it does not yield any uncertainty information. As this model runs relatively quickly, it was chosen as an example to illustrate a Dakota/MELCOR coupling to support uncertainly analysis using a Bayesian approach. Bayesian calibration is an iterative process that yields a distribution of an uncertain parameter that is consistent with the experimental data. There are some disadvantages to performing Bayesian analysis. Tens of model evaluations may be required to properly converge the resulting MCMC chain and it is not possible to determine how many samples are needed to converge the chain before sampling begins; it is only apparent if the chain is converged when analyzing the results. To aid in the Bayesian process, a surrogate was constructed and coupled to Dakota (instead of MELCOR) using the Gaussian process method in Dakota. The surrogate was created from a large sweep (480 sampled values of c_{torque} for all ZS-1 air experiments) of sampled values. 240 samples were held back initially to test the surrogate quality on the remaining 240 points; the maximum error between the surrogate and the MELCOR value was less than 0.25%, which indicated a good quality surrogate on the c_{torque} range sampled.

Once the surrogate was constructed, performing the Bayesian calibration and obtaining enough samples to build the MCMC chain was relatively straightforward. Figure 3.9 shows the MCMC chain mean c_{torque} value (excluding an initial burn-in period) that demonstrates good convergence and the distribution of the c_{torque} value, which has a mean value of 0.3467. This is similar to the value obtained from the determinist calibration, however, this parameter includes uncertainty information. The parameter uncertainty can then be propagated to uncertainty in the model turbine speed and torque results.

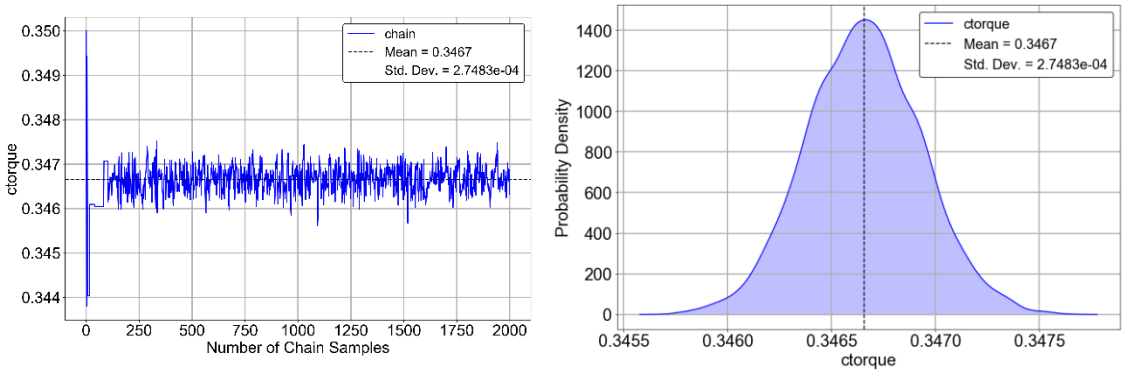

Figure 3.9: Bayesian calibration MCMC chain and distribution on ctorque (burn-in period 1000 samples).

Loss data for the GS-2 has not been provided at the time of writing this report, so it was not practical at this time to perform a similar exercise. However, by using the same values obtained from the ZS-1 calibration, it can be observed from the plots in Figure 3.10 and Figure 3.11 that the same coefficients are likely not appropriate for the GS-2 air modeling. This is significant, as during the FY19 modeling, which used a different modeling implementation of the RCIC turbine, it was observed that it might be possible for the same coefficient values to be used with the different turbines. The FY19 report [20] did however also note that the parameters may be unidentifiable. If GS-2 loss data (as a function of turbine speed) or another quantity that would fix the loss coefficient becomes available, it will be possible to repeat the calibration exercise with the GS-2 and compare the data determined loss coefficients and the calibration determined c_{torque} coefficients.

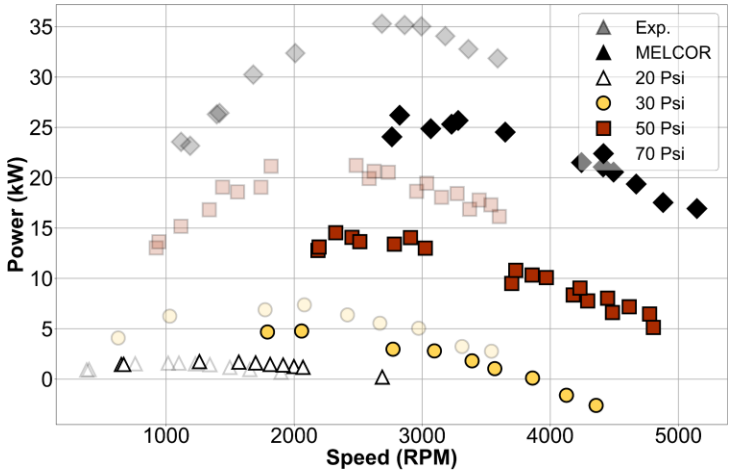

Figure 3.10: GS-2 air test turbine power vs speed curves for the experiments and the calibrated results using ctorque and loss coeffiecients from the ZS-1 data.

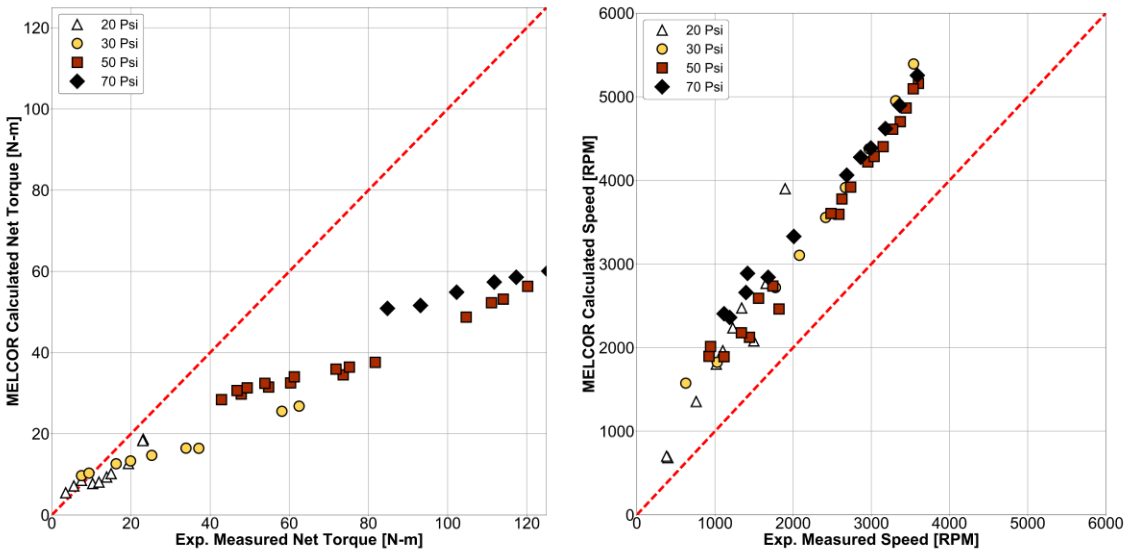

Figure 3.11: The experimental data vs the MELCOR results for the GS-2 air tests using ctorque and loss coeffiecients from the ZS-1 data.

3.3.2. Generic BWR Modeling Results

Several self-regulation modes have been observed for the generic BWR RCIC turbopump system:

- **Stable-degraded self-regulation**: Stable mode of self-regulation that is characterized by constant turbine speed and stable, yet degraded, pump injection.
- **Unstable self-regulation**: Unstable mode of self-regulation that is characterized by significant or frequent fluctuations to both the RCIC turbine speed and injection rate.
- **Semi-stable degraded self-regulation**: Degraded, yet stable mode of self-regulation characterized by a steady turbine speed, but with possible significant fluctuations of turbine speed and pump injection rate.

The different self-regulating modes and model parameters found to influence them are the focus of the results presented in these next sections. To aid in discussion of these topics, results of several simulations will be shown to characterize the dynamic feedback between the RCIC system flow conditions and the RCIC response. As the feedback is coupled and dynamic, changes to turbine, pump, or general inputs cause changes in behavior that are difficult to isolate. Several trends will be discussed in more detail.

Figure 3.12 includes plots of the RCIC speed vs time for the three observed self-regulating modes. For all model results shown in this section, RCIC is assumed to start (controlled) operation approximately 60 s into the simulation and battery power is depleted at 2 hours. Most of these models used a c_{torque} value of 1.0; if a different value was used, it will be described in the results. During controlled operations, the mass flow rate through the RCIC turbine is approximately ~18,000 lbm/hr (8165 kg/hr) steam. Once the battery power is depleted, the governor and trip values fail to a full-open position. The sudden increase in governor valve flow area causes a large, sudden increase in the steam admittance to the RCIC turbine. This in turn causes an initial overshoot of the turbine and an increase in the pump injection rate at 2 hours. The increased turbine speed and pump injection ceases when the RPV water level rises significantly (due to the increased

RCIC injection) and the steam intake for the RCIC turbine begins to take in water, which has an adverse effect on turbine performance. The adverse performance is caused by increased losses associated with the turbine ingesting water and a decrease in drive torque from the turbine inflow nozzles due to the significant decrease in imparted momentum of the water jets compared to a supersonic steam jet. After the initial overspeed of the RCIC turbine and overflow of the ingest to the RCIC steam line, the RCIC turbopump system enters into a regulating mode, as described in Section 3.2.2.2.

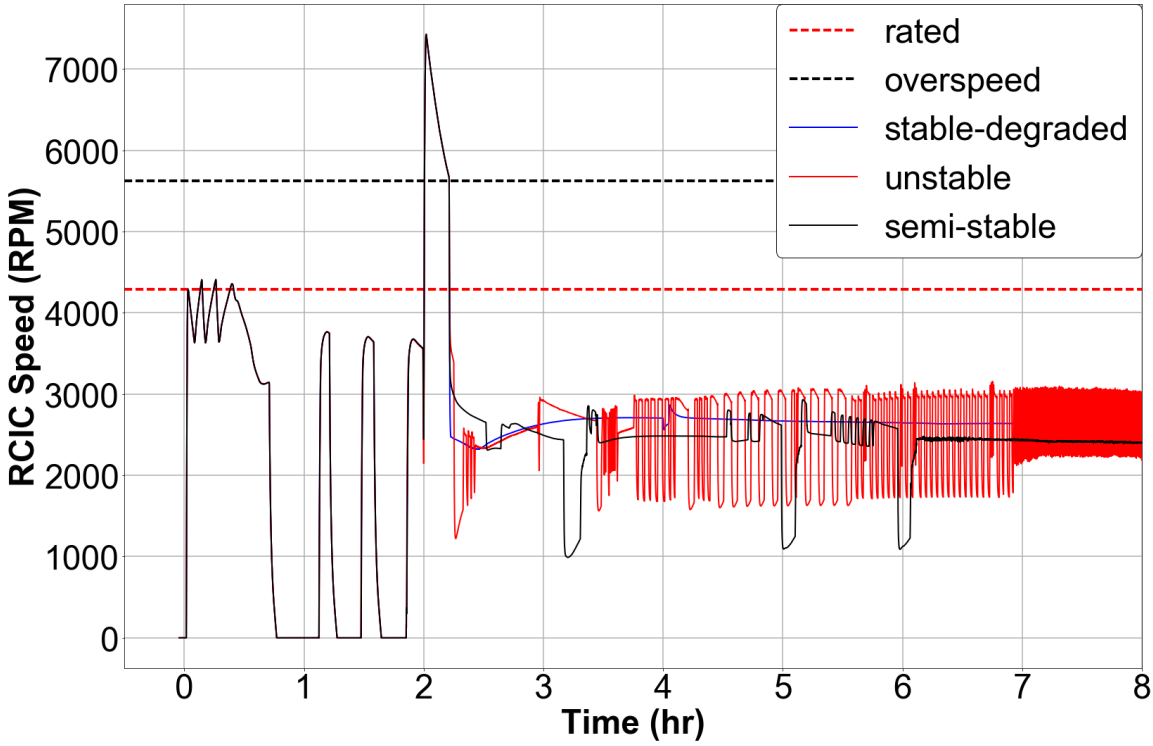

Figure 3.12: Generic BWR observed self-regulating modes summary turbine speed plot.

The stable degraded self-regulation mode is characterized by a steady turbine speed without significant or frequent fluctuations of turbine speed and pump injection rate. This is illustrated in Figure 3.13, Figure 3.14, Figure 3.15, and Figure 3.16, which show the RCIC turbine speed, pump injection rate, RPV water level, and RCIC nozzle void. The behavior seen in the RCIC speed plot is the turbopump system maintained a degraded, but stable mode of operation. The pump is rated at 38.7 kg/s, however while running in self-regulating mode, the pump injected at a rate between ~13 and ~18 kg/s. The RPV water level is maintained relatively steady during the self-regulating mode, such that the bottom elevation of the steam line intake is underwater (Figure 3.15). The nozzle void plot shows that bottom three nozzles (nozzles 3, 4, and 5) are always completely submerged, nozzle 2 is submerged for the majority of the calculation, and nozzle 1 is uncovered throughout the modeling.

There is uncertainty in the most appropriate method to model the nozzle elevation for the GS-1. The GS-1 nozzle and steam chest geometry are such that the nozzles are arranged at different elevations in a "C-like" configuration where all nozzles are arranged in a serial fashion. However, it is unknown how the mixture of steam and water will behave once it enters the steam nozzle bank. For example, it is unknown if lower elevations in the steam bank will accumulate water or

if the steam and water mixture will preferentially flow through nozzles based on their arrangement rather than elevation (i.e., does the first nozzle in the series pass more mass than the final nozzle in the series?). The FY19 [20] modeling of Fukushima Daiichi Unit 2's RCIC turbine steam chest used a single nozzle flow path that combined all nozzle areas and set the nozzle flow path height accordingly. Therefore, the water level in the steam chest determined the percent area of the nozzle flow path that was submerged.

The modeling performed for the FY20 stable degraded self-regulating mode implemented 5 nozzle paths, each with the same area corresponding to a 0.5 inch throat diameter, arranged equidistant in terms of flow path elevation along the height of the steam chest control volume. It was noted during the FY20 modeling that the frequency and magnitude of the RCIC turbine speed fluctuations were highly sensitive to the nozzle inputs that influence preferential phasic flow (gas or liquid preferred) and also the nozzle elevation. For the FY21 results, the phasic flow preference was not set to either gas or liquid preferential (and instead determined by MELCOR according to flow path conditions). Figure 3.17 is a plot of the steam chest water height compared to the nozzle heights. The water height in the steam chest stays relatively stable as a result of a relatively RPV water level, with the exception of the drop in water elevation that starts at 10.3 hours. This drop in water elevation is due to the decrease in RCIC turbine speed at this time, which then picks up speed again after the pump source changes from the CST to the wetwell at 12.7 hours. The top nozzle remains uncovered, which admits a steady amount of steam to the turbine and maintains a steady pump rate that is high enough to prevent the steam intake line from totally uncovering, but low enough to prevent complete submersion of the steam line intake.

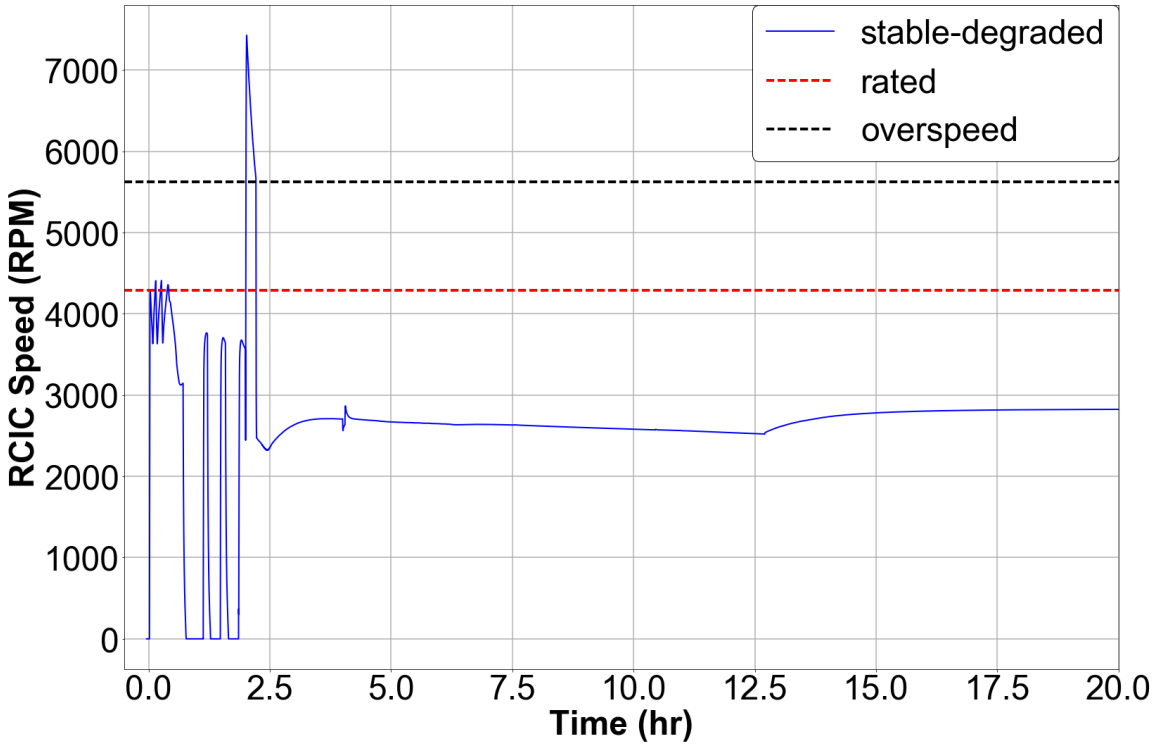

Figure 3.13: Stable degraded self-regulating mode RCIC turbine speed plot.

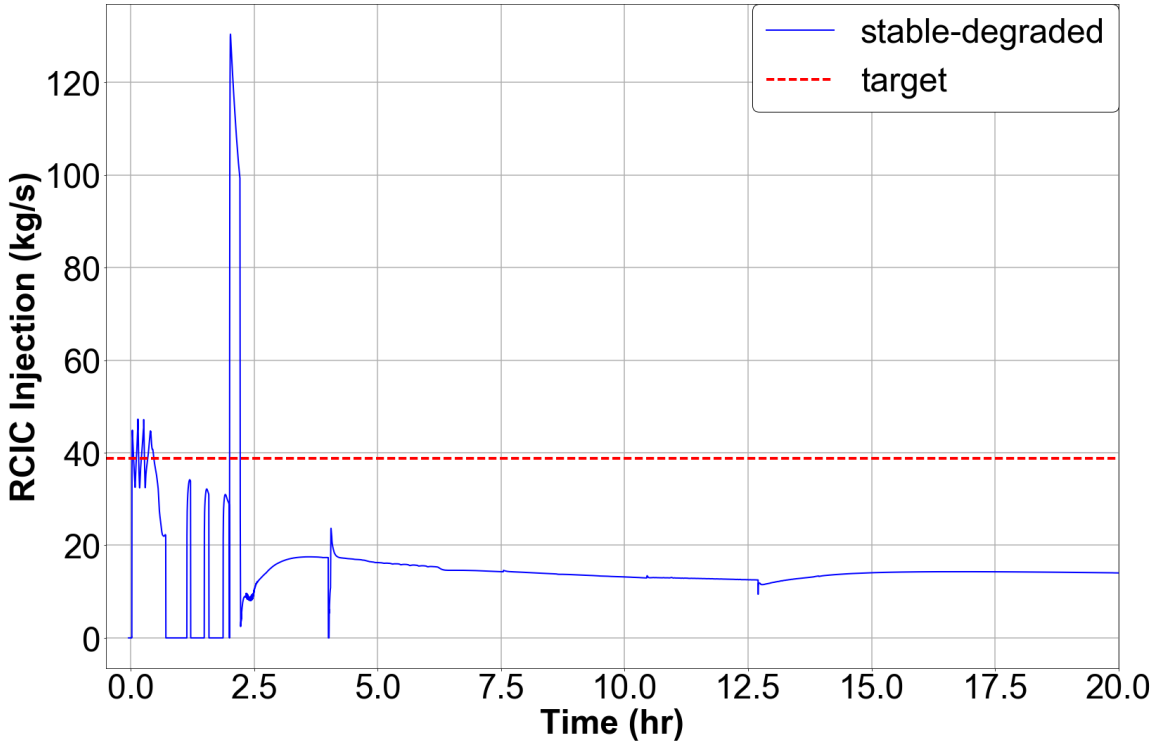

Figure 3.14: Stable degraded self-regulating mode RCIC pump injection rate.

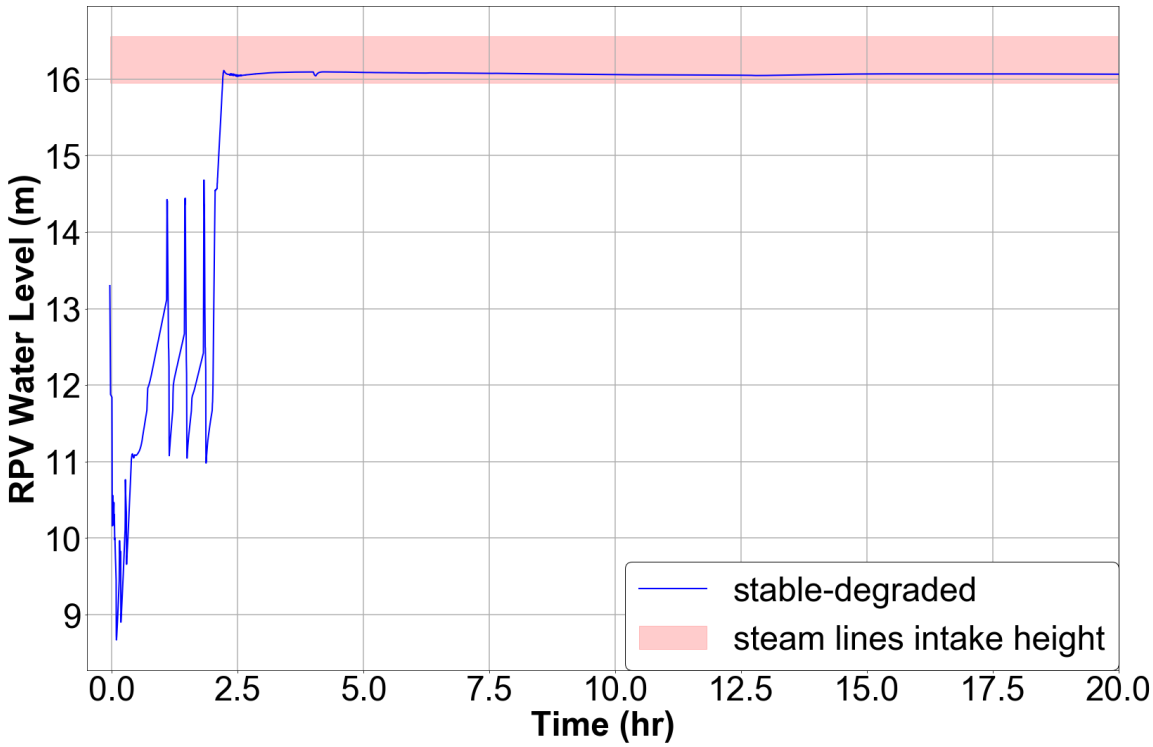

Figure 3.15: Stable degraded self-regulating mode RPV water level plot.

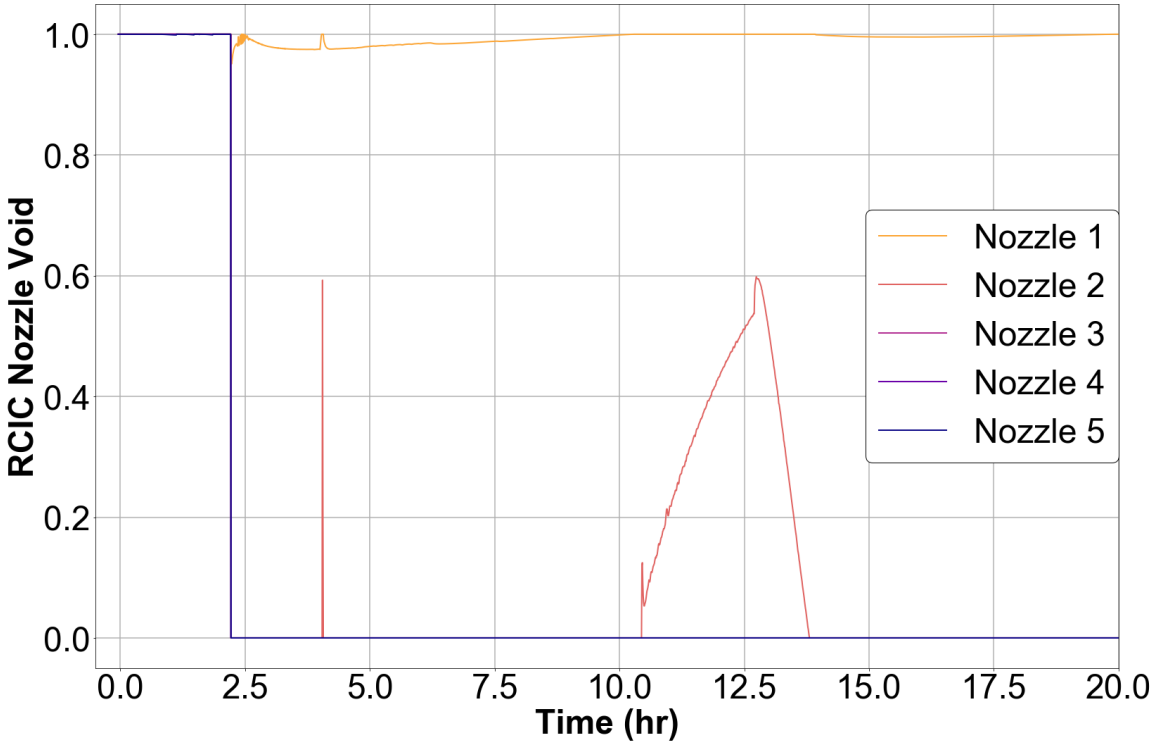

Figure 3.16: Stable degraded self-regulating mode RCIC nozzle void.

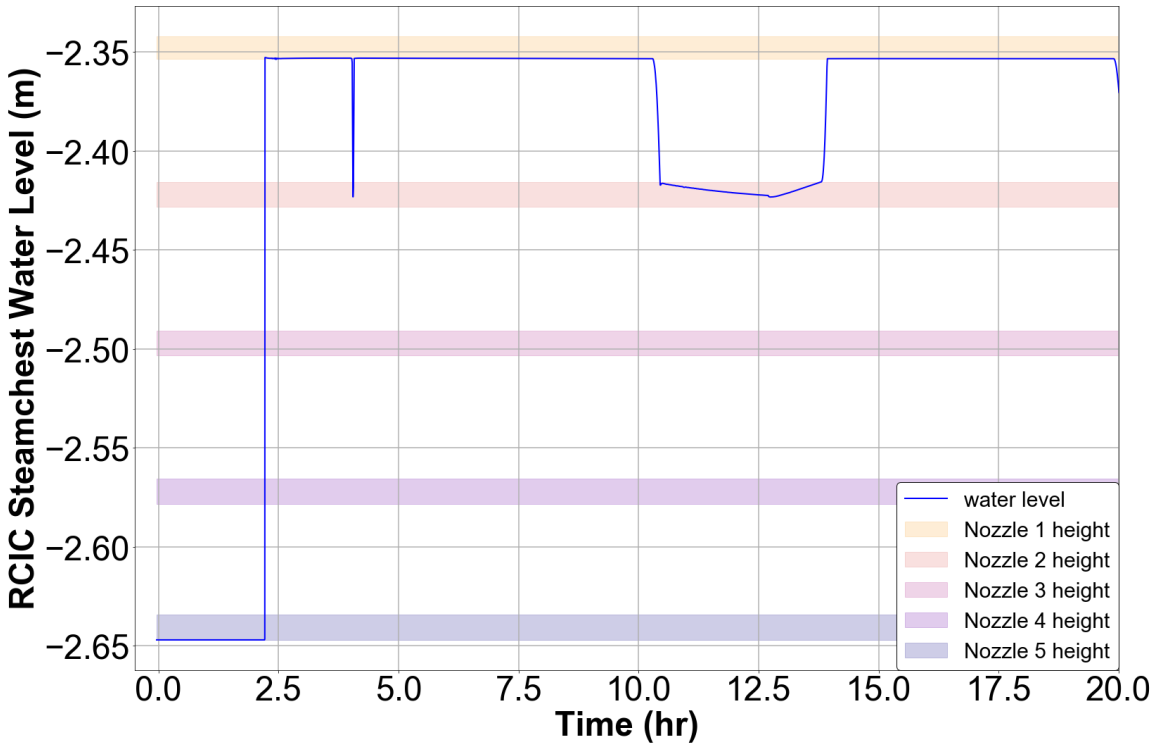

Figure 3.17: Stable degraded self-regulating mode steam chest water height compared to the RCIC nozzle height.

The unstable self-regulation mode is characterized by frequent and significant fluctuations to the turbine speed and pump injection rate. This is illustrated in Figure 3.18, Figure 3.19, Figure 3.20, and Figure 3.21 which show the RCIC turbine speed, pump injection rate, RPV water level, and RCIC nozzle void. The behavior seen in the RCIC speed plot is a degraded and unstable mode of operation. The pump injection rate fluctuates frequently and it reaches high injection rates when the RPV/steam chest water level are low and the turbine ingests more steam.

The original (pre-FY20 RCIC modifications) generic BWR modeling split the nozzle into three high and two low nozzles that were located at the top and bottom of the steam chest. This same input implementation of the nozzle elevations was adopted here: three high and two low. The nozzles would preferentially flow steam (high nozzles) or water (low nozzles) based on the water level in the steam chest control volume. After the loss of battery power and the onset of steam line flooding, lower nozzles continually flow water while higher nozzles flow a fluctuating mixture of steam and water. This resulted in the transient RCIC turbine behavior seen in Figure 3.19. This change in behavior from the stable degraded self-regulation was caused solely by this input change; all nozzles were still modeled separately, and their areas remained the same. Comparing the steam chest water level and nozzle height for the two cases shows that while the bottom nozzles in both cases flow water during self-regulating mode, the stable degraded case only has a single nozzle flowing steam for the majority of the calculation, in contrast to the unstable case which has three nozzles passing a mixture of steam and water. Spikes in the steam admittance to the turbine and the associated fluctuations to the turbine driving momentum results in the unstable turbine and injection behavior seen in the unstable case.

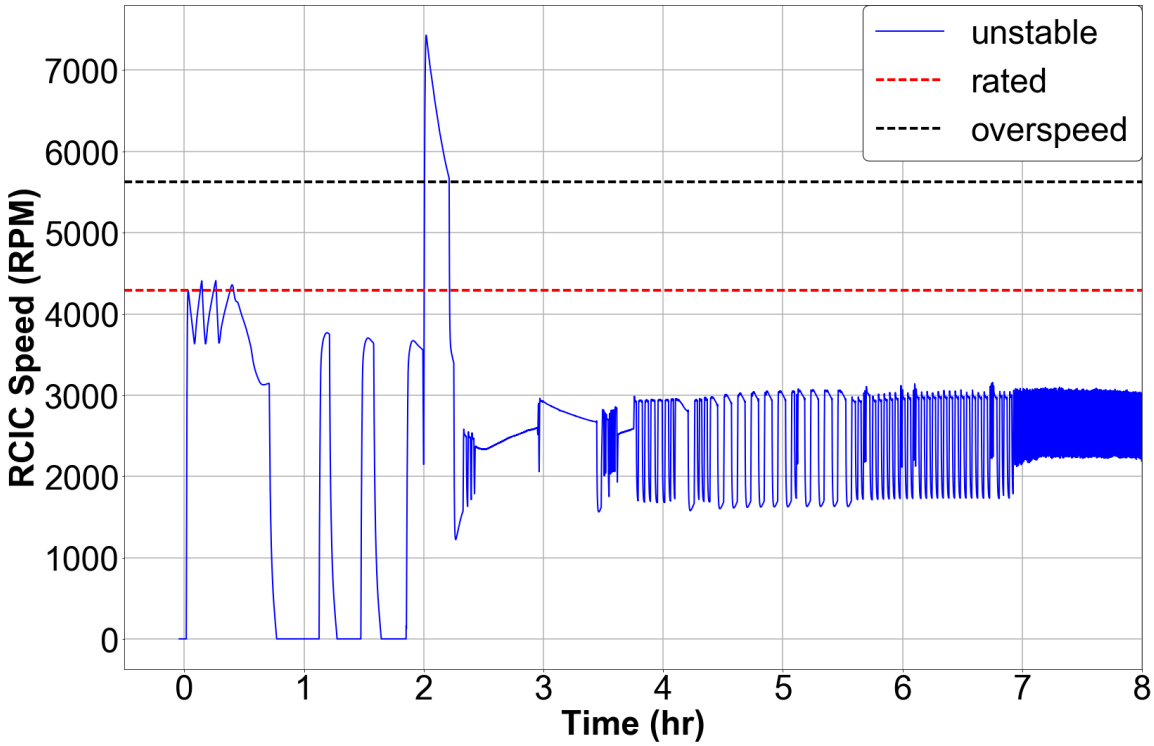

Figure 3.18: Unstable self-regulating mode RCIC turbine speed plot.

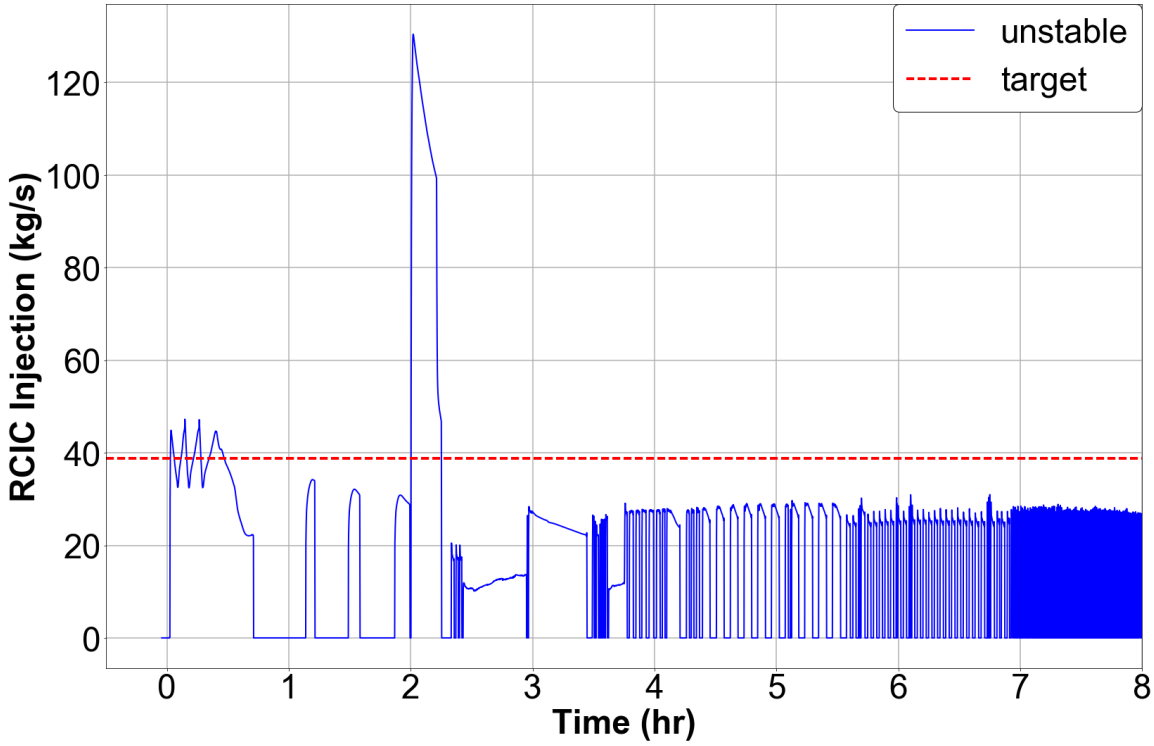

Figure 3.19: Unstable self-regulating mode RCIC pump injection rate.

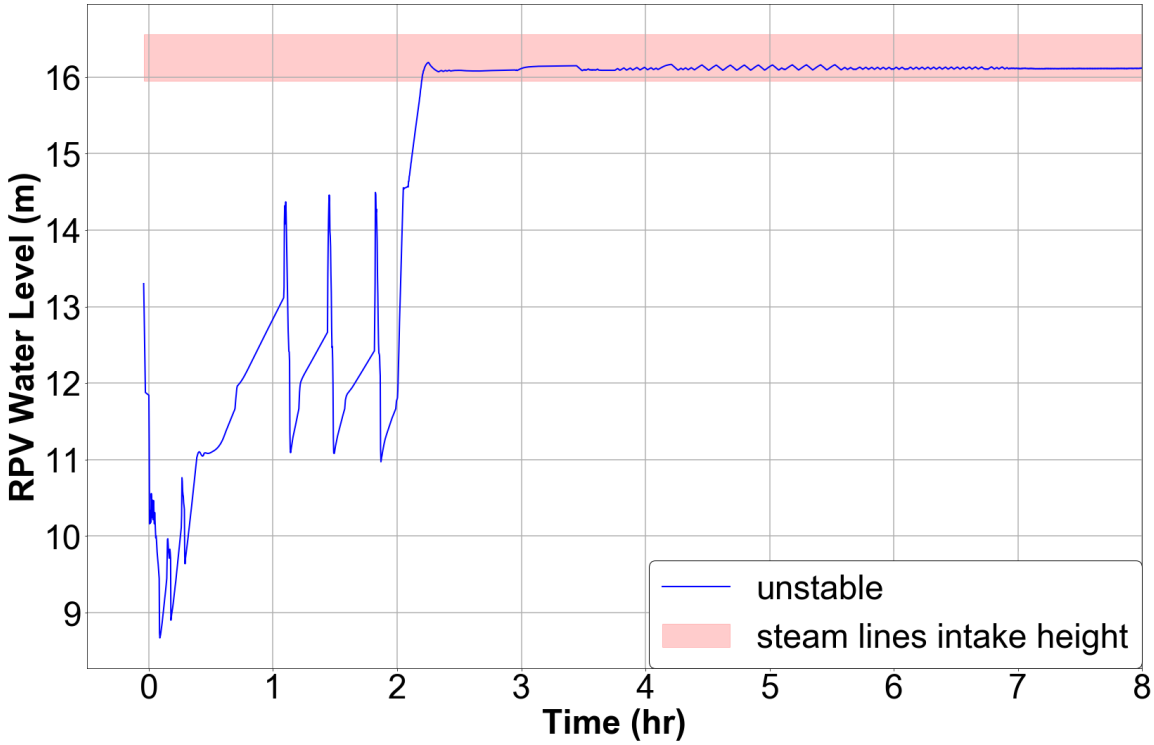

Figure 3.20: Unstable self-regulating mode RPV water level plot.

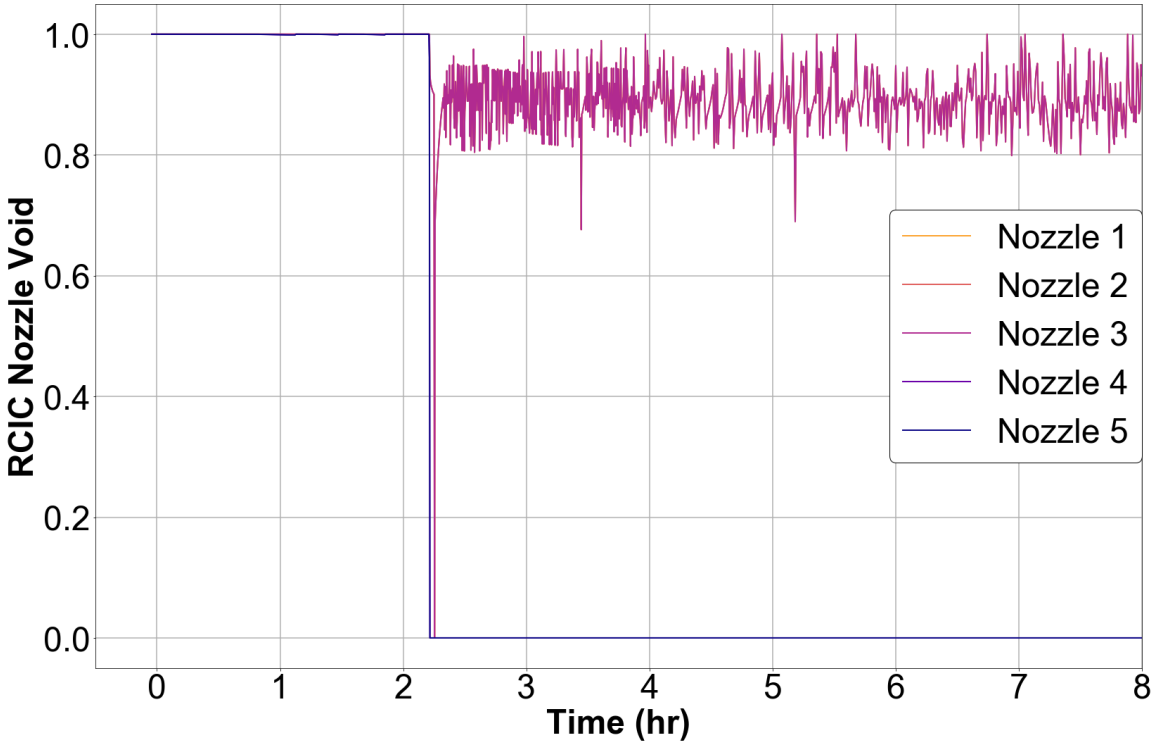

Figure 3.21: Unstable self-regulating mode RCIC nozzle void.

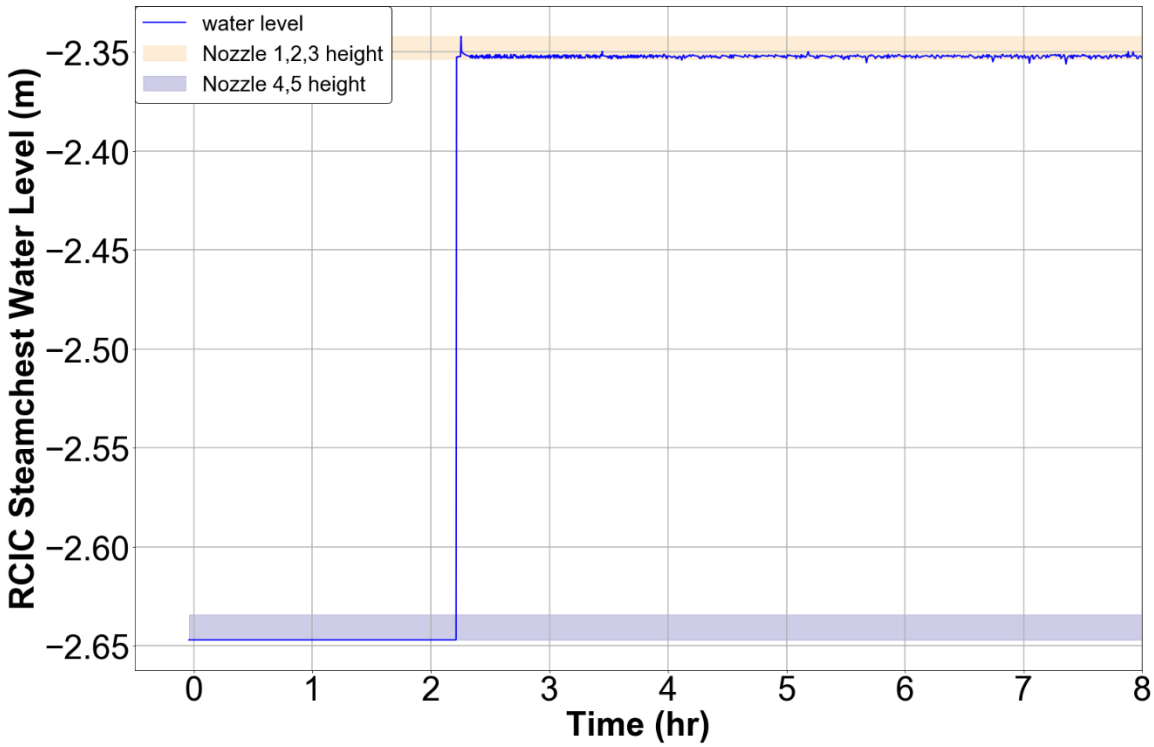

Figure 3.22: Unstable self-regulating mode steam chest water height compared to the RCIC nozzle height.

The semi-stable degraded self-regulation mode is characterized by a relatively stable turbine speed, but frequent and significant fluctuations to the turbine speed and pump injection rate. This is illustrated in Figure 3.23, Figure 3.24, Figure 3.25, and Figure 3.26 which show the RCIC turbine speed, pump injection rate, RPV water level, and RCIC nozzle void. This modeling used a modified version of the unstable self-regulation mode input deck, however, the nozzles were split into two high and three low nozzles that were located at the top and bottom of the steam chest (compared to three high and two low in the unstable case). Similar to before, the nozzles would flow steam (high nozzles) or water (low nozzles) based on the water level in the steam chest control volume. These results interestingly have characteristics of both the stable and unstable self-regulating modes. The addition of an extra low nozzle results in a greater quantity of water mass flowing through the turbine. The momentum contributed by the water nozzles is less than the steam nozzles due to the jet velocities. There are also losses associated with water injection into the turbine as windage is assumed to scale with density and the water jets may impose drag on the turbine wheel depending on the wheel speed. The reduction of the "high" nozzles by one prevents as large of steam admittance spikes (compared to the unstable self-regulation) that cause wide swings in turbine performance. However, due to the split in the nozzle elevations, the turbine will experience fluctuations in water flow, which distinguishes it from the gradual changes in nozzle void fraction seen in the stable-degraded input.

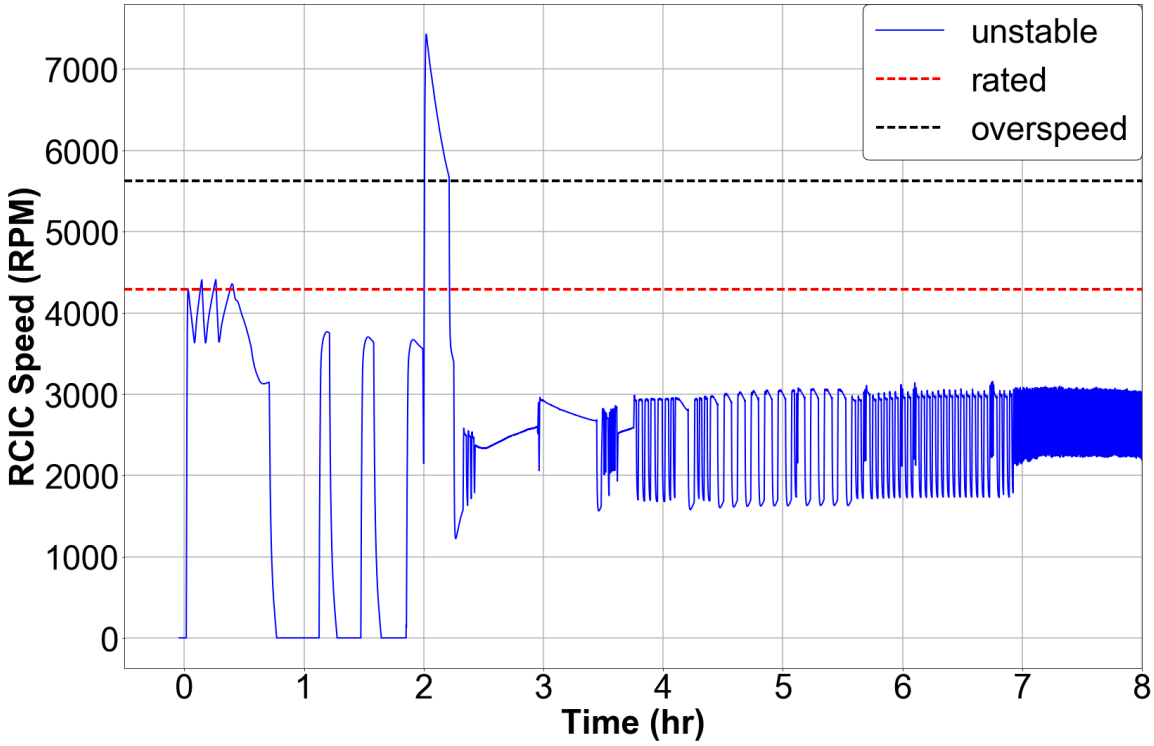

Figure 3.23: Semi-stable self-regulating mode RCIC turbine speed plot.

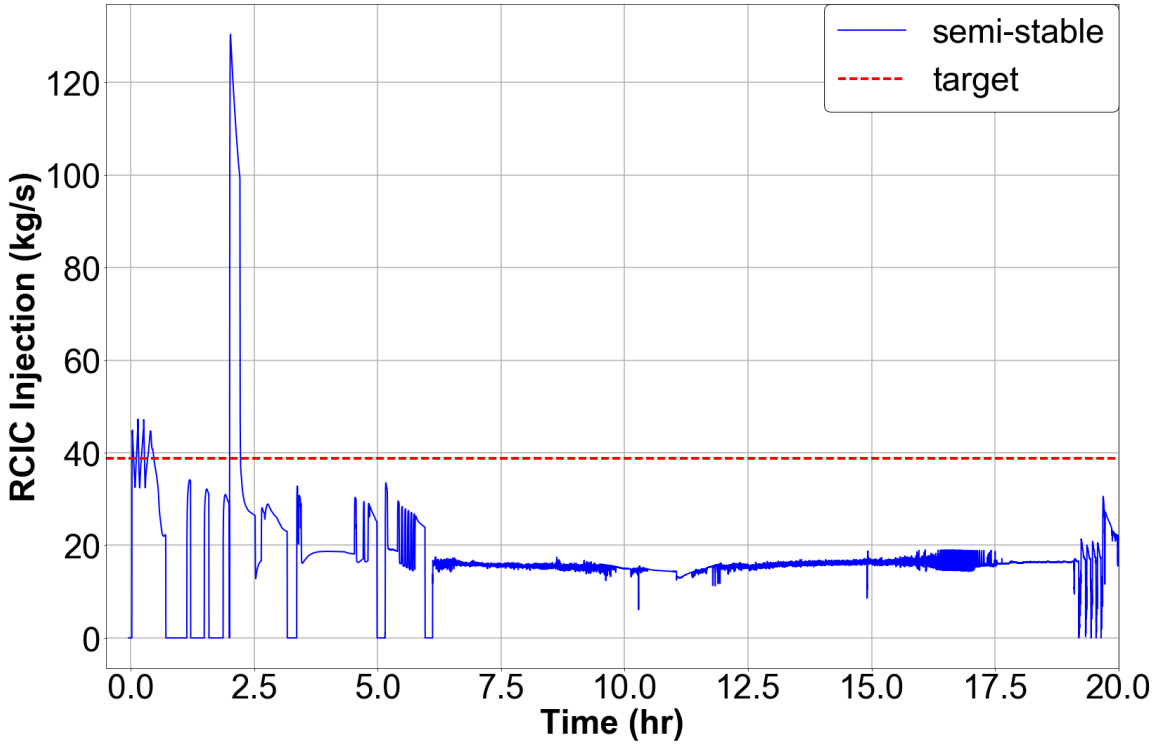

Figure 3.24: Semi-stable self-regulating mode RCIC pump injection rate.

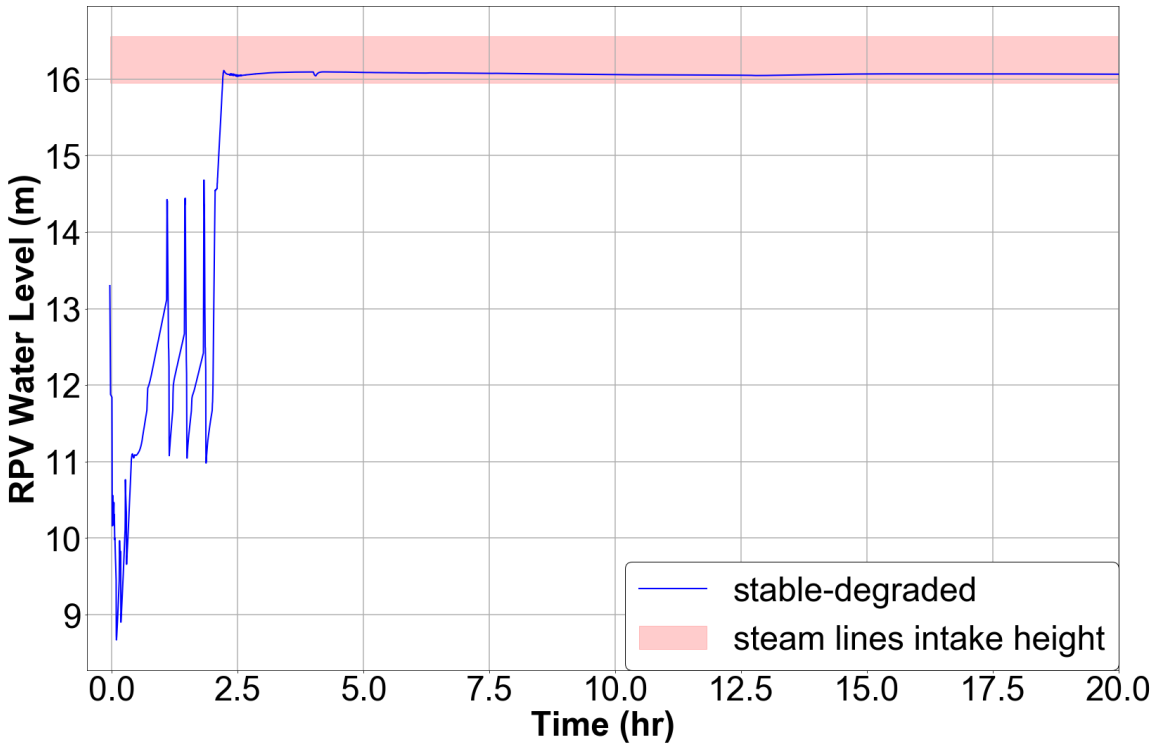

Figure 3.25: Semi-stable self-regulating mode RPV water level.

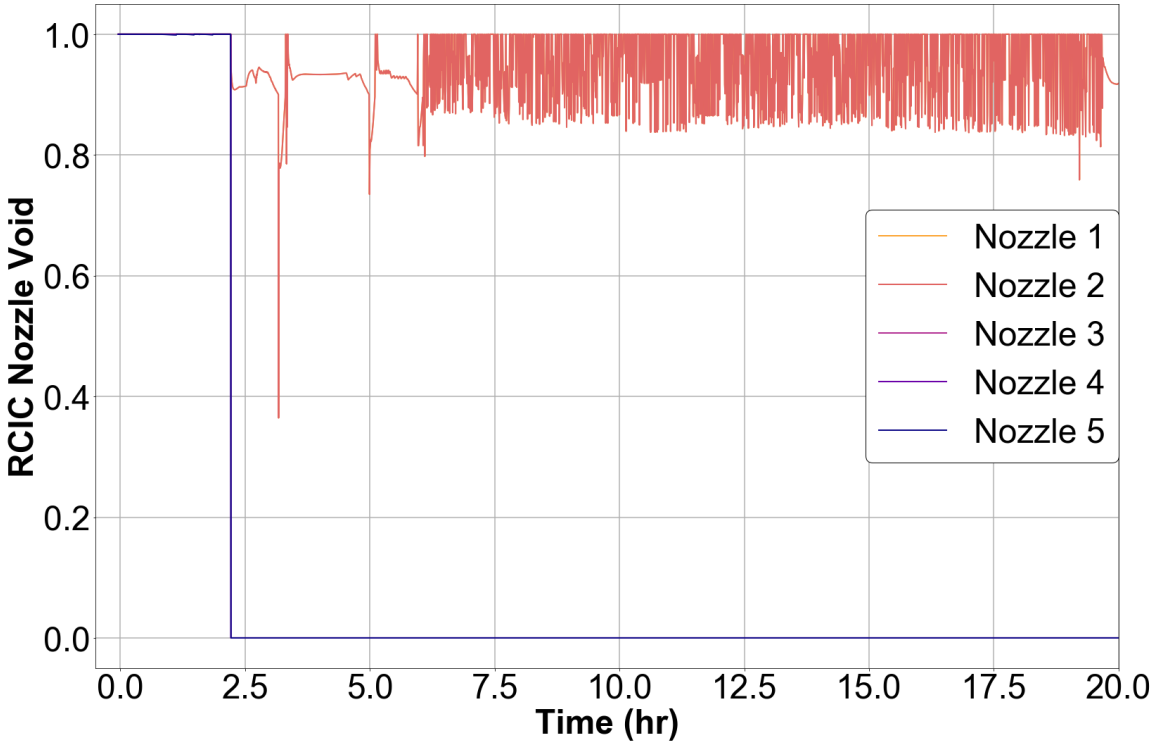

Figure 3.26: Semi-stable self-regulating mode RCIC nozzle void.

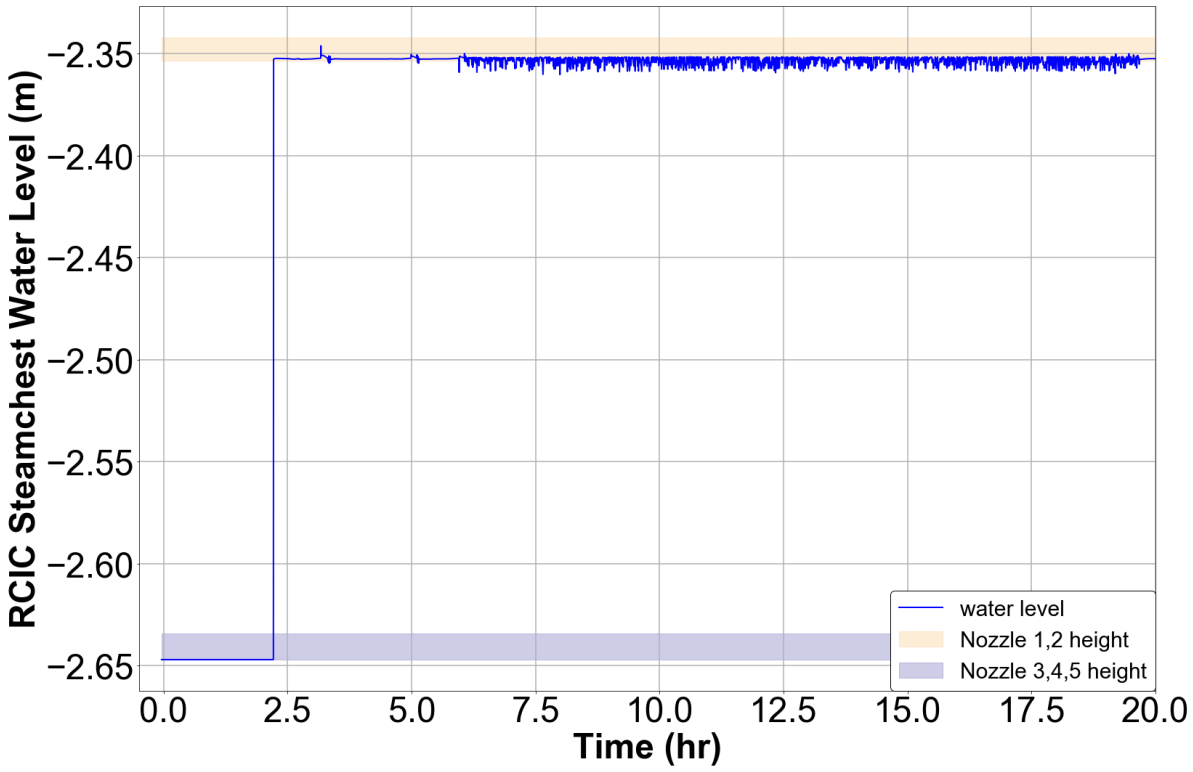

Figure 3.27: Semi-stable self-regulating mode steam chest water height compared to the RCIC nozzle height.

Interestingly, though it was possible to drive the current inputs using $c_{windage}$ = 1.0 and controlled turbine steam mass flow rate ~18,000 lb/hr to different self-regulating behavior, it was not possible at the time of writing and after many model iterations to recreate another distinctive self-regulating behavior that was observed using a slightly older MELCOR input. The older turbine used $c_{windage}$ =2.53 and had a controlled turbine steam mass flow rate of approximately 10,000 lb/hr. The older turbine produced significantly more torque from an equivalent amount of mass (compared to the newer input implementation). Figure 3.28, Figure 3.29, Figure 3.30, and Figure 3.31 show the $c_{windage}$=2.53 case RCIC turbine speed, pump injection rate, RPV water level, and RCIC nozzle void. As the turbine produced significantly more torque from an equivalent intake of steam and water, this resulted in much larger swings of turbine speed and injection magnitude, even compared to the new unstable self-regulation mode. Figure 3.32 shows the steam chest height compared to the nozzle elevations for this case. In this case, the bottom 4 nozzles flowed water (similar to the stable degraded case). Nozzle 1 however flowed alternating slugs of steam and water. Many input iterations were applied on the new input deck to attempt to recreate this specific mode, however we were unsuccessful at recreating it. This further demonstrates how sensitive the self-regulating behavior is to model inputs. Small changes in uncertain inputs have large implications for modeling results and behavior of the systems.

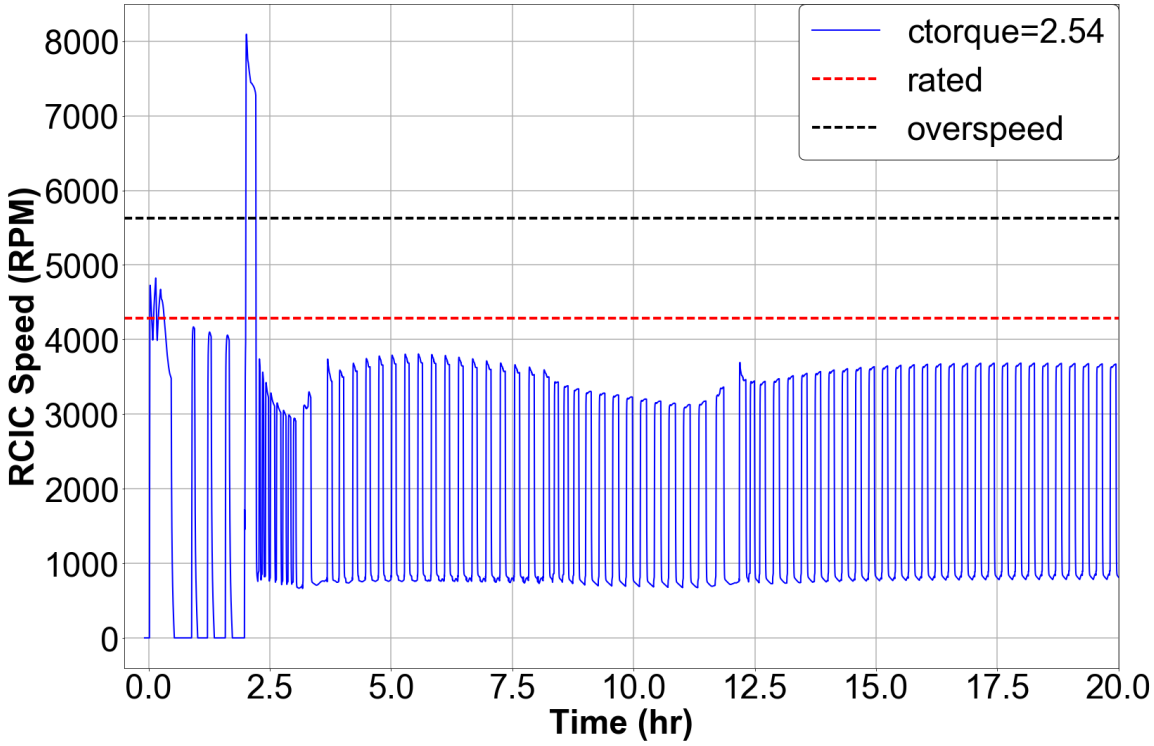

Figure 3.28: Ctorque = 2.53 modeling self-regulating mode RCIC turbine speed.

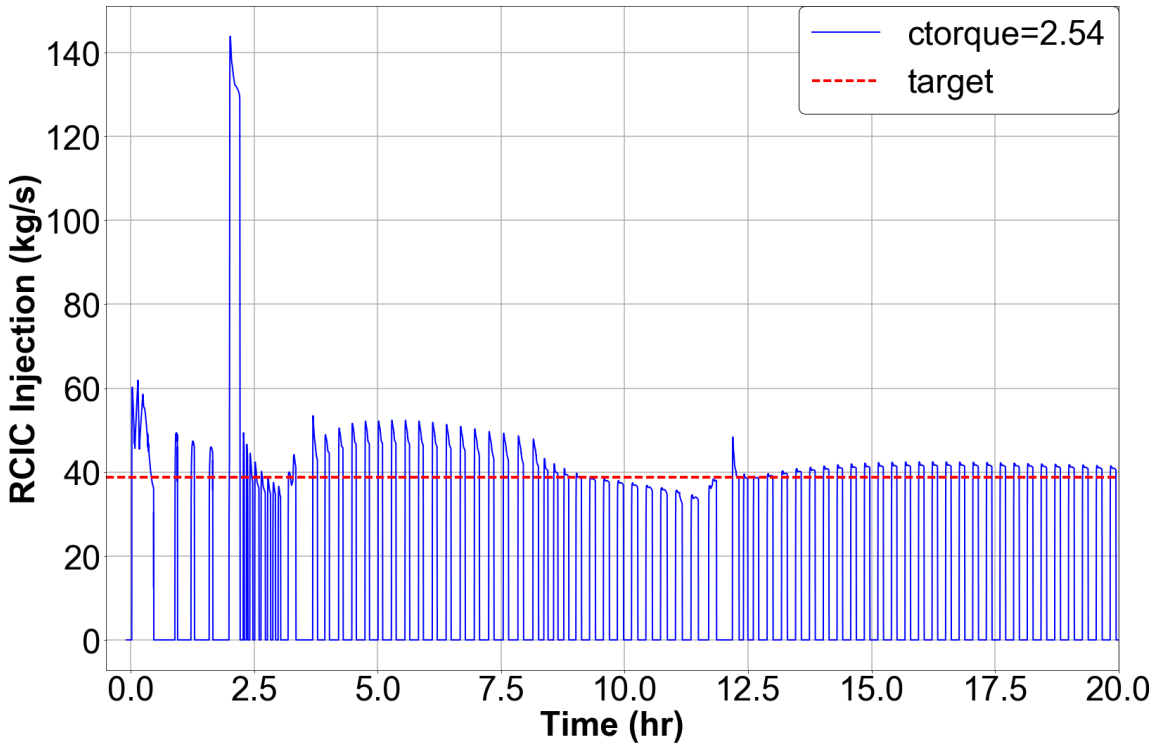

Figure 3.29: Ctorque = 2.53 modeling unstable self-regulating mode pump injection rate.

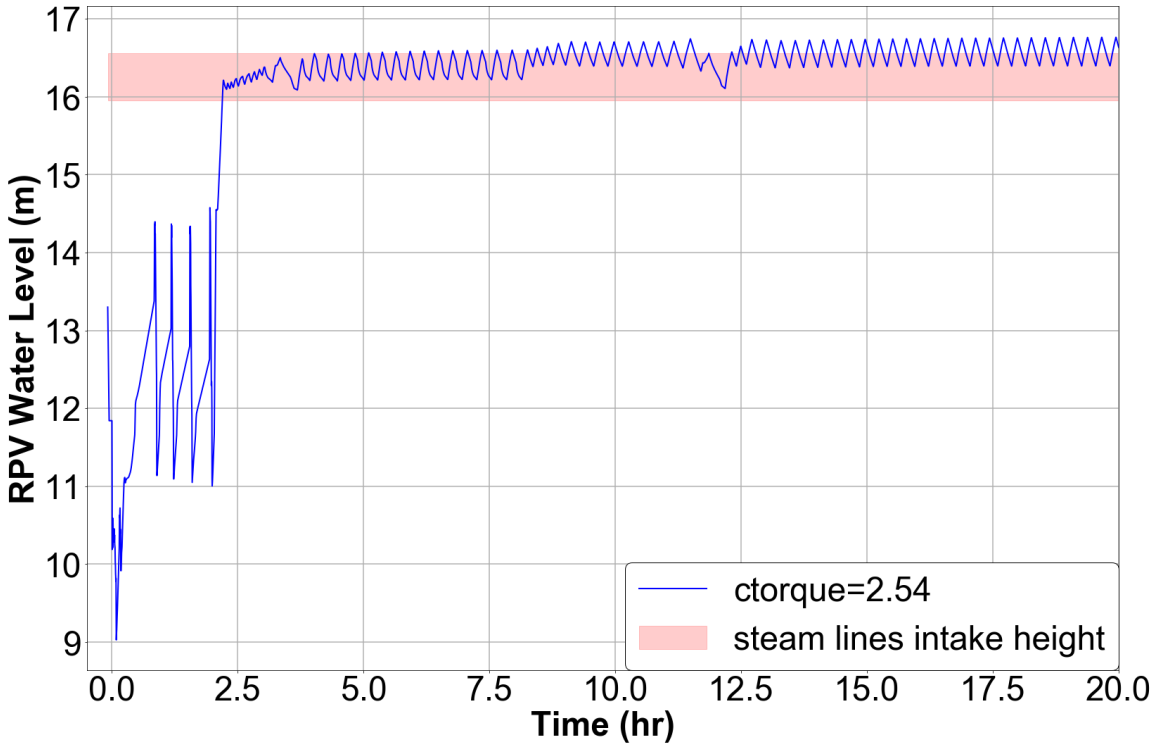

Figure 3.30: Ctorque = 2.53 modeling unstable self-regulating mode RPV water level.

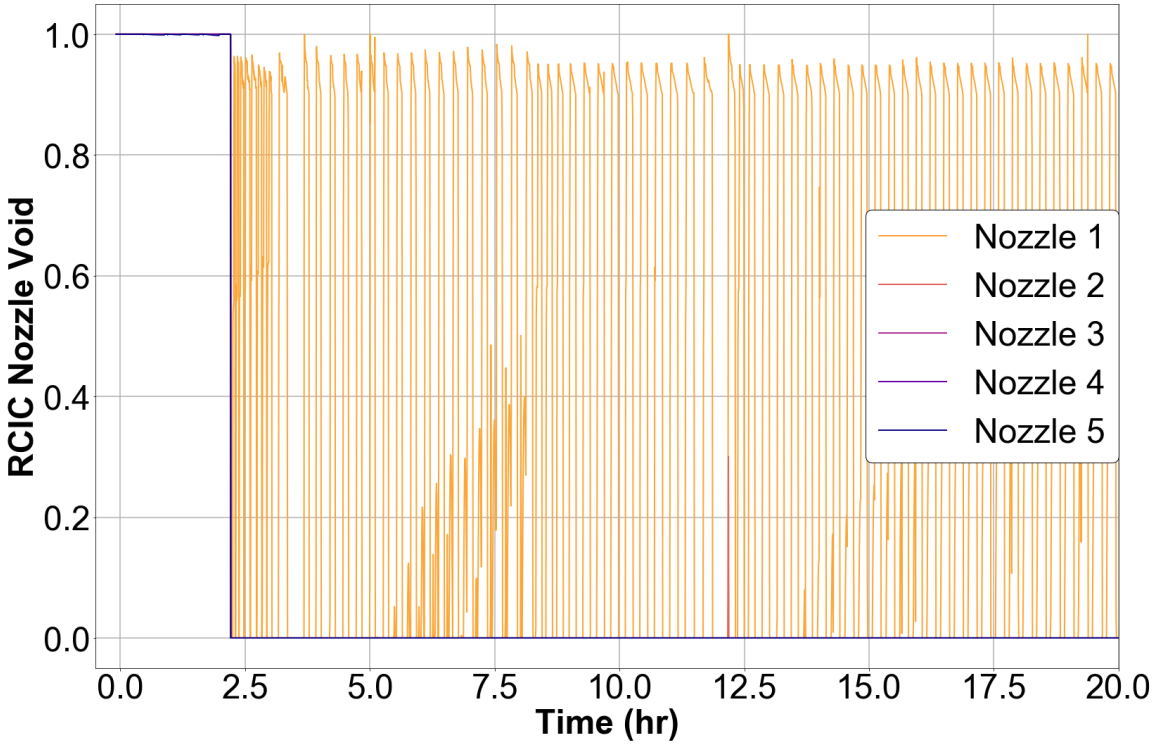

Figure 3.31: Ctorque = 2.53 modeling unstable self-regulating mode RCIC nozzle void.

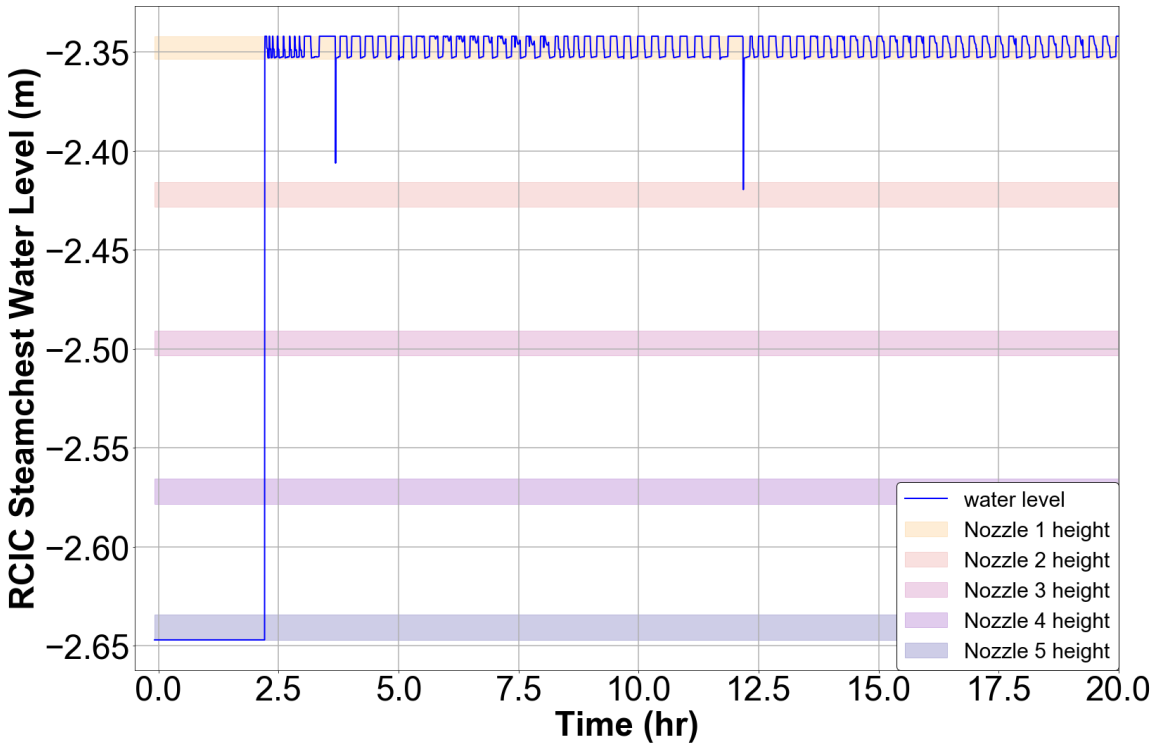

Figure 3.32: Ctorque = 2.53 modeling steam chest water height compared to the RCIC nozzle height.

4. SUMMARY

In the extended FY21 period-of-performance, SNL continued its milestone 7 modeling and simulation activities by improving:

- MELCOR input models of TAMU experiments, and
- MELCOR input models for a generic BWR

Experimental turbine loss data was used to inform the MELCOR input model of the TAMU ZS-1 experiment. By calibrating the torque multiplier that accompanies MELCOR mechanistic models, good agreement with TAMU ZS-1 experimental data was demonstrated and a recommended torque multiplier (for ZS-1 applications) was obtained. A similar study could be repeated with the GS-2 turbine as soon as experimental data becomes available.

The generic BWR input model employing the latest mechanistic MELCOR RCIC physics models was used to investigate the nature of Terry turbine self-regulation under loss of electrical power. Several distinct modes of self-regulating behavior were detected. The predicted response is apparently a strong function of user modeling choices especially with respect to Terry turbine nozzles and upstream steam line piping. Experimental insights from the TAMU GS-2 test matrix could influence MELCOR user input modeling methodology in this respect.

REFERENCES

[1] Severe Accident Analysis Department, *Terry Turbopump Expanded Operating Band Summary of Program Plan – Revision 1*, SAND2017-5562, Sandia National Laboratories, Albuquerque, NM, May 2017.

[2] Osborn, D., M. Solom, K. Ross, and J. Cardoni, *Terry Turbopump Expanded Operating Band Full-Scale Component Experiments and Basic Science Detailed Test Plan – Revision 2*, SAND2017-10773, Sandia National Laboratories, Albuquerque, NM, September 2017.

[3] International TTEXOB Charter, Version 5.3, July 14, 2017.

[4] Kirkland, K. V. (Principal Investigator), *Terry Turbopump Expanded Operating Band*, Year 2 Technical Report, Research Agreement No. M1702670, Project Period June 1, 2017 – March 30, 2019, Reporting Period June 1, 2017 – March 30, 2019.

[5] Solom, M., D. Osborn, N. Andrews, *Terry Turbopump Expanded Operating Band Experimental Efforts in Fiscal Year 2019 – Progress Report*, Sandia Letter Report, Sandia National Laboratories, Albuquerque, NM, August 2019.

[6] Kirkland, K. V. (Principal Investigator), *Terry Turbopump Expanded Operating Band*, Year 1 Technical Report, Research Agreement No. M1702670, Project Period June 1, 2017 – July 31, 2019, Reporting Period June 1, 2017 – March 30, 2018.

[7] Osborn, D., Solom, M., Ross, K., Kirkland, K. V., Patil, A., Tsuzuki, N., *Terry Turbine Expanded Operating Band: Initial Experimental Efforts*, SAND2018-6511C, 2018 ANS Winter Meeting Embedded Topical on Advances in Thermal Hydraulics (ATH 2018), November 11-15, 2018, Orlando, FL, USA.

[8] Solom, M. and Osborn, D., *Terry Turbopump Expanded Operating Band Experimental – Fiscal Year 2018 Progress Report*, SAND2018-9907, Sandia National Laboratories, Albuquerque, NM, September 2018.

[9] Andrews, N., Gilkey, L., Solom, M., *Using Terry Turbine Systems for Enhancing Plant Resilience*, SAND2019-8966 PE, Sandia National Laboratories, Albuquerque, NM, 2019.

[10] Patil, A., Sundar, S., Wang, Y., Solom, M., Kirkland, K. V., Morrison, G., *Characterization of Steam Impulse Turbine for Two-Phase Flow*, International Journal of Heat and Fluid Flow, Volume 79, October 2019, https://doi.org/10.1016/j.ijheatfluidflow.2019.108439

[11] Patil, A., Wang, Y., Solom, M., Alfandi, A., Sundar, S., Kirkland, K. V., Morrison, G., *Two-Phase Operation of a Terry Turbine using Air and Water Mixtures as Working Fluids*, Applied Thermal Engineering, Volume 165, January 2020. https://doi.org/10.1016/j.applthermaleng.2019.114567

[12] National Electrical Manufacturers Association (NEMA), NEMA SM23, *Steam Turbines for Mechanical Drive Service*.

[13] Gauntt, R., et al., *Fukushima Daiichi Accident Study (Status as of April, 2012)*, SAND2012-6173, Sandia National Laboratories, Albuquerque, NM, August 2012.

[14] Ross, K., et al, *Modeling of the Reactor Core Isolation Cooling Response to Beyond Design Basis Operations – Phase 1*, SAND2015-10662, Sandia National Laboratories, Albuquerque, NM, December 2015.

[15] “ＭＡＡＰコードによる炉心・格納容器の状態の推定”, http://www.tepco.co.jp/nu/fukushima-np/images/handouts_120312_02-j.pdf

[16] *MAAP Code-based Analysis of the Development of the Events at the Fukushima Daiichi Nuclear Power Station*, http://www.tepco.co.jp/en/nu/fukushima-np/images/handouts_120312_04-e.pdf

[17] Barrett, K. E., *Sales Aid Memo #12, Terry Wheel Water Slug Test*, The Terry Steam Turbine Company, 1973.

[18] Cardoni, J., K. Ross, and D. Osborn, *Terry Turbopump Analytical Modeling Efforts in Fiscal Year 2017 – Progress Report*, SAND2018-4533, Sandia National Laboratories, Albuquerque, NM, May 2018.

[19] Cardoni, J., Ross, K., Osborn, D., *Terry Turbopump Analytical Modeling Efforts in Fiscal Year 2018 – Progress Report*, SAND2018-10133, Sandia National Laboratories, Albuquerque, NM, September 2018.

[20] L. Gilkey, M. Solom, N. Andrews, Terry Turbopump Expanded Operating Band Modeling and Full-Scale Test Development Efforts in Fiscal Year 2019 – Progress Report, SAND2019-13423, Sandia National Laboratories, Albuquerque, NM, October 2019.

[21] Terry Turbine Expanded Operating Band Advisory Committee, Terry Turbine/RCIC ExOB Hybrid Milestone White Paper, Rev. 1, April 2020.

[22] K. Kirkland. Terry Turbopump Expanded Operating Band Full-Scale Component and Basic Science Testing and Analysis Program. Progress Report. May 1 – July 31, 2020.

[23] MELCOR Computer Code Manuals, Volume 1: Primer and Users’ Guide, Version 2.2. NUREG/CR-6119. Sandia National Laboratories.

[24] MELCOR Computer Code Manuals, Volume 2: Reference Manual, Version 2.2. NUREG/CR-6119. Sandia National Laboratories

[25] L. Gilkey, B. Beeny, M. Solom, Terry Turbopump Expanded Operating Band Modeling and Full-Scale Test Development Efforts in Fiscal Year 2020 – Progress Report, SAND2020-9368, Sandia National Laboratories, Albuquerque, NM, October 2020.

[26] B. Adams et al., “Dakota, A Multilevel Parallel Object-Oriented Framework for Design Optimization, Parameter Estimation, Uncertainty Quantification, and Sensitivity Analysis: Version 66.12 User’s Manual”. SAND2020-12495, Sandia National Laboratories, Albuquerque, NM, 2020.

FURTHER READING

[27] Osborn, D., Solom, M., Terry Turbopump Expanded Operating Band Full-Scale Integral Long-Term Low-Pressure Experiments – Preliminary Test Plan, SAND2018-12965, Sandia National Laboratories, Albuquerque, NM, January 2019.

[28] Lomperski, S., Farmer, M., Kilsdonk, D., and Aeschlimann, R. *Multidimensional Flow and Heat Transport Natural Convection Test Facility, Preliminary Design Summary, DRAFT*, Nuclear Engineering Division, Argonne National Laboratory, April 18, 2005.

[29] Tarbell, W., Brockmann, J., Pilch, M., Ross, J., Olier, M., Lucero, D., Kerley, T., Arellano, F., and Gomez, R. *Results from the DCH-1 Experiment*, NUREG/CR-4871, SAND86-2483, Sandia National Laboratories, May 1987.

[30] Qiu, A., Pena, M., Fuentes, D., and Chan, J. *Scaled Experiment of Fukushima Unit 2 Self Regulating Feedback*, undergraduate senior design final report, Department of Nuclear Engineering, Texas A&M University, College Station, TX, May 2019.

[31] Kelso, J. et al., *Terry Turbine Maintenance Guide, RCIC Application*, EPRI Technical Report Number 1007460, Electric Power Research Institute, Palo Alto, CA, 2012.

[32] Zucker, R. D., Biblarz, O., *Fundamentals of Gas Dynamics*, John Wiley & Sons, Inc., Hoboken, NJ, 2002.

[33] Ross, K., Cardoni, J., and Osborn, D., *Terry Turbopump Analytical Modeling Efforts in Fiscal Year 2016 – Progress Report*, SAND2018-4337, Sandia National Laboratories, Albuquerque, NM, April 2018.

[34] Kirkland, K., *Quality Assurance Plan for RCIC Testing at Texas A&M University*, August 2017.

[35] Light Water Reactor Sustainability Program, *Quality Assurance Plan Description*, INL/MIS-10-19844 Revision 2, U.S. Department of Energy, July 2016.

[36] Avincola, V. A., Jessup, W., *Trip Report for Texas A&M Site Visit and Technical Advisory Committee Meeting*, 0140-0361-TR-001, prepared for: Electric Power Research Institute, Inc., MPR Associates, Inc., Alexandria, VA., 2019.

[37] Walker, T. (EPRI Project Manager), *Terry Turbine Expanded Operating Band Program Review*, 3002015508 Draft A, Electric Power Research Institute, Palo Alto, CA, 2019.

[38] Tsuzuki, N., D. T. Nguyen, and Y. Hassan, *Result of Freejet Testing*, presented at the Nuclear Maintenance Applications Center Terry Turbine Users Group Meeting, July 10-12, 2018, Albuquerque, NM.

[39] Tsuzuki, N., Chaki, M., Nguyen, D. T., Hassan, Y. A., Kirkland, K. V., *Flow Behavior Observation of Single-Phase Air Jet Simulating a Nozzle of Terry Turbine Using PIV*, Transactions of the American Nuclear Society 119

[40] Maher, B., Nguyen, D. T., Madozinhos, C., Tomaz, G., Hassan, Y., *Turbulent Flow Measurements of the Under-Expanded Free Jet and Jet Impinging on a Flat Surface*, Transactions of the American Nuclear Society 120, 997-1000.

[41] International Electrotechnical Commission, *Industrial Process-Control Valves – Part 2-3: Flow Capacity – Test Procedures*, IEC 60534-2-3:2015, Edition 3.0, December 2015.

[42] Miller, G. H., United States District Court, Southern District of Texas, Houston Division, *Dresser-Rand Company v. Schutte & Koerting Acquisition Company, et al.*, Civil Action H-12-184, Memorandum Opinion, February 13, 2012.

[43] Terry Steam Turbine Company, *Emergency Feedwater Pump Turbine*, Vendor Manual 00036-000, Crystal River 3 Vendor Technical Manual, Revision 16.

[44] Ingersoll Rand, *Emergency Feedwater Pump*, Progress Energy Nuclear Engineering Crystal River – Unit 3, Vendor Manual 00108-000, Revision 28, 2010.

[45] The Terry Steam Turbine Co., Hartford, CT, *Terry Instruction Manual Type Z-1 and ZS-1*, 1959.

[46] Luthman, Nicholas Gerard Jr., *Evaluation of Impulse Turbine Performance Under Wet Steam Conditions*, Master's Thesis, Texas A&M University, 2017. Available electronically from http://hdl.handle.net/1969.1/161659.

[47] Nguyen, D. T., B. Maher, Y. Hassan, *Effects of Nozzle Pressure Ratio and Nozzle-to-Plate Distance to Flowfield Characteristics of an Under-Expanded Jet Impinging on a Flat Surface*, Aerospace 2019, 6, 4, January 2019. https://doi.org/10.3390/aerospace6010004

[48] Nguyen, T., B. Maher, Y. Hassan, *Flowfield Characteristics of a Supersonic Jet Impinging on an Inclined Surface*, AIAA Journal, Vol. 58 No. 3, March 2020. https://doi.org/10.2514/1.J058897

[49] Peck, D. J., *Turbine Oil Degradation and its Effects on Performance of a Terry Turbine in Nuclear Applications*, Master's Thesis, Texas A&M University, 2019. Available electronically from http://hdl.handle.net/1969.1/187526.

[50] Zhang, W., D. Wang, A. Renganathan, H. Zhang, *Modeling and Assessment of Two-Phase Transonic Steam Flow with Condensation through the Convergent-Divergent Nozzle*, Nuclear Engineering and Design, Vol. 364, August 2020. https://doi.org/10.1016/j.nucengdes.2020.110632

[51] Vandervort, J., G. Lukasik, B. Ayyildiz, M. Solom, A. Delgado, K. V. Kirkland, A. Patil, *Performance Evaluation of a Terry GS-2 Steam Impulse Turbine with Air-Water Mixtures*, Applied Thermal Engineering, Vol. 191, 2021. https://doi.org/10.1016/j.applthermaleng.2021.116636

[52] Charrouf, M., B. Jessup, Memorandum Re: *Preliminary Review of Plant Data and RCIC Expanded Operating Band Test Data Assessment*, MPR Associates, Inc., 0140-0393-MEMO-001, Rev. 0, June 22, 2020.

[53] Kirkland, K. V. (Principal Investigator), *Terry Turbopump Expanded Operating Band*, Final Technical Report, Research Agreement No. M1702670, Project Period June 1, 2017 – December 31, 2019, Reporting Period April 1, 2019 – December 27, 2019.

[54] Terry Turbine Expanded Operating Band Advisory Committee, *Terry Turbine/RCIC ExOB Hybrid Milestone White Paper*, Rev. 1, April 2020.

[55] K. Vierow Kirkland, A. Delgado, Y. A. Hassan, T. D. Nguyen, A. R. Patil, Terry Turbopump Expanded Operating Band-Full-Scale Component and Basic Science Testing at Texas A&M University, draft Comprehensive Technical Report, prepared for The Idaho National Laboratory under Battelle Energy Alliance Award # 183672, June 8, 2021.

This page left blank

DISTRIBUTION

Email—Internal

Name	Org.	Sandia Email Address
Matthew Solom	06812	msolom@sandia.gov
Bradley Beeny	08852	babeeny@sandia.gov
David Luxat	08852	dlluxat@sandia.gov
Lindsay Gilkey	08853	lngilke@sandia.gov
Technical Library	01977	sanddocs@sandia.gov

Email—External (encrypt for OUO)

Name	Company Email Address	Company Name
Hongbin Zhang	hongbin.zhang@inl.gov	Idaho National Laboratory

This page left blank

This page left blank

Sandia National Laboratories

Sandia National Laboratories is a multimission laboratory managed and operated by National Technology & Engineering Solutions of Sandia LLC, a wholly owned subsidiary of Honeywell International Inc. for the U.S. Department of Energy's National Nuclear Security Administration under contract DE-NA0003525.